Electronic Supplementary Material (ESI) for Organic & Biomolecular Chemistry.

Supporting Information for

Mannich-Type Addition of 1,3-Dicarbonyl Compounds to Chiral *tert*-Butanesulfinyltrifluoroacetaldimines. Mechanistic Aspects and Chiroptical Studies

Giuseppe Mazzeo, Giovanna Longhi; Sergio Abbate, Francesca Mangiavacchi, Claudio Santi, Jianlin Han, Vadim A. Soloshonok, Luca Melensi, Renzo Ruzziconi

Table of contents

S1 Experimental. Section

S2 General Procedure for the addition of dicarbonyl compounds **2a-e** to (S_s)-*N*-*tert*-butanesulfinyltrifluoroacetaldimine in solvent free condition at 70 °C.

S3 General procedure for the of DBU catalyzed addition of dicarbonyl compounds **2a-e** to (S_s)-*N*-*tert*-butanesulfinyltrifluoroacetaldimine in dichloromethane at −10 °C.

S6 Original spectra of new compounds.

S32 Chirooptical properties.

S33 Assignment of the absolute configuration of diastereomers (X,S_s)-**3a** and (Y,S_s)-**3a**

S33 Comments on the VCD-IR, ORD and ECD analysis and computational methods for the assignment of the absolute configuration.

S41 Electronic Circular Dichroism (ECD) and ORD analysis.

S44 References.

Experimental Section

Unless otherwise specified, ^{1}H NMR and ^{13}C NMR spectra were recorded at 400 and 100 MHz, respectively, in $CDCl_3$ solution using tetramethylsilane as an internal standard. ^{19}F NMR spectra were recorded at 376 MHz in $CDCl_3$ solution using $CFCl_3$ as a reference standard. IR spectra were registered in $CHCl_3$ solution in the 4000–625 cm^{-1} range. HRMS spectra were registered on Agilent Technologies 6540 UHD Accurate Mass Q-TOF LC/MS. The purity of all final products was attested by either elemental analyses performed on Carlo Erba Elemental Analyzer Mod. 1106 or HMRS determinations.

General procedure for the addition of dicarbonyl compounds ***2a-e*** *to (S)-N-tert-butanesulfinyltrifluoroacetaldimine in solvent free condition at 70 °C.*

(*S*)-*tert*-butanesulfinyltrifluoroacetaldimine (0.62 g, 3.0 mmol) was mixed with 1,3-dicarbonyl compound **2a-e** (1.1 eq) in a screw-cap vial and the mixture, was heated in an oil bath at 70 °C until the minor reagent was completely disappeared. After cooling, the crude was taken up with dichloromethane (1-2 mL) and the resulting solution was charged at the top of a SiO_2 column and eluted with 60:40 v/v mixture of CH_2Cl_2/EtOAc, after a portion was first analyzed by ^{19}F NMR in order to determine the diastereomeric ratio (dr). The isolated products were characterized as follow.

(*R*,*S*$_s$)-2-Acetyl-*N*-(*tert*-butanesulfinyl)-3-oxo-1-(trifluoromethyl)butylamine [(*R*,*S*$_s$)-3a]. White solid, m.p. 132–134 °C; ^{1}H NMR δ 5.19 (d, *J* = 8.3 Hz, 1 H), 4.49 (m, 1 H), 4.04 (d, *J* = 4.4 Hz, 1 H), 2.36 (s, 3 H), 2.35 (s, 3 H), 1.24 (s, 9 H). ^{13}C NMR δ 205.0, 199.6, 124.9 (q, *J* = 281 Hz), 63.3, 58.6 (q, *J* = 30 Hz), 57.4, 32.6, 30.1, 22.8 (3 C). ^{19}F NMR δ –74.88 (d, *J* = 7.4 Hz, 3 F). Elem. A. calcd. for $C_{11}H_{18}F_3NO_3S$ (301,32): C, 43.85; H, 6.02; N, 4.65; Found: C, 43.79; H, 6.09; N, 4.71.

Methyl (*A*,*R*,*S*$_s$)- and (*B*,*R*,*S*$_s$)-2-acetyl-3-amino-*N*-(*tert*-butanesulfinyl)-4,4,4-trifluorobutyrate [(*A*,*R*,*S*$_s$)- and (*B*,*R*,*S*$_s$)-3b]. Sticky solid, mixture of two epimers. (*A*,*R*,*S*$_s$)-**3b**: ^{1}H NMR δ 5.58 (d, *J* = 9.3 Hz, 1 H), 4.5 (m, 1 H), 4.01 (d, *J* = 2.5 Hz, 1 H), 3.89 (s, 3 H), 2.39 (s, 3 H), 1.25 (s, 9 H); ^{13}C NMR δ 203.7, 166, 6, 124.8 (q, *J* = 281 Hz), 59.8 (q, *J* = 31 Hz), 57.3, 54.1, 32.8, 22.8 (3 C); ^{19}F NMR δ –74.67 (d, *J* = 7.9 Hz, 3 F). (*B*,*R*,*S*$_s$)-**3b**: ^{1}H NMR δ 5.30 (d, *J* = 9.3 Hz, 1 H), 4.52 (m, 1 H), 3.87 (s, 3 H), 3.76 (d, *J* = 3.1 Hz, 1 H), 2.36 (s, 3 H), 1.25 (s, 9 H); ^{13}C NMR δ 198.2, 169, 5, 124.8 (q, *J* = 280 Hz), 58.0 (q, *J* = 31 Hz), 57.0, 56.3, 29.4, 22.7 (3 C); ^{19}F NMR δ –75.47 (d, *J* = 7.9 Hz, 3 F). HRMS: calcd for $C_{11}H_{18}F_3NO_4S$, 317.0909; found, 317.0903.

(*A*,*R*,*S*$_s$)- and (*B*,*R*,*S*$_s$)-2-Acetyl-*N*-(*tert*-butanesulfinyl)-3-oxo-3-phenyl-1-(trifluoromethyl)-propylamine (3c). 1.5:1 mixture of two epimers A and B (A/B = 1.5). (*A*,*R*,*S*$_S$)-**3c**: white crystals, m.p. 125–127 °C; ^{1}H NMR δ 7.96 (d, *J* = 7.7 Hz, 2 H), 7.67 (t, *J* = 7.5 Hz, 1 H), 7.54 (t, *J* = 7.5 Hz, 2 H), 5.71 (d, *J* = 8.1 Hz, 1 H), 4.88 (d, *J* = 3.0 Hz, 1 H), 4.66 (quint.d, *J* = 8.0 and 3.0 Hz, 1 H), 2.25 (s, 3 H), 1.25 (s, 9 H); ^{13}C NMR δ 199.5, 197.8, 137.0, 135.2, 129.7, 129.0, 125.1 (q, *J* = 280 Hz), 59.7 (q, *J* = 31 Hz), 57.4, 56.9, 30.2, 22.8;

^{19}F NMR δ –74.37 (d, *J* = 7.8 Hz, 3 F). (B,R,S_S)**-3c**. ^{1}H NMR δ 7.98 (d, *J* = 7.5 Hz, 2 H), 7.65 (t, *J* = 7.5 Hz, 1 H), 7.52 (t, *J* = 7.4 Hz, 2 H), 4.95 (d, *J* = 6.4 Hz, 1 H), 4.52 (quint, *J* = 6.3 Hz, 1 H), 4.36 (d, *J* = 8.8 Hz, 1 H), 2.29 (s, 3 H), 1.23 (s, 9 H); ^{13}C NMR δ 202.7, 196.0, 136.5, 134.9, 129.7, 129.2, 124.8 (d, *J* = 281 Hz), 58.3 (q, *J* = 30 Hz), 57.5, 57.3, 30.2, 22.8; ^{19}F NMR δ –74.91 (d, *J* = 7.0 Hz, 3 F). Elem. A. calcd for $C_{16}H_{20}F_3NO_3S$ (363,40): C, 52.88; H, 5.55; N, 3.85; Found: C, 52.72; H, 5.47; N, 3.91.

(S,S_s)**-2-Benzoyl-*N*-(*tert*-butanesulfinyl)-3-oxo-3-phenyl-1-(trifluoromethyl)propylamine** **[**(S,S_s)**-3d]**. ^{1}H NMR δ 8.02 (d, *J* = 7.2 Hz, 4 H), 7.58 (t, *J* = 7.2 Hz, 2 H), 7.51 (t, *J* = 7.7 Hz, 4 H), 5.92 (d, *J* = 3.4 Hz, 1 H), 5.87 (d, *J* = 8.0 Hz, 1 H), 4.59 (quint.d, *J* = 8.0 and 3.4 Hz, 1 H), 1.24 (s, 9 H); ^{13}C NMR δ 194.9, 191.7, 136.6, 135.1, 134.8, 134.7, 129.7, 129.5, 129.2, 128.8, 125.0 (q, *J* = 280 Hz), 59.4 (q, *J* = 30 Hz), 57.4, 52.2, 22.8; ^{19}F NMR δ –74.05 (d, *J* = 7.7 Hz, 3 F). Elem. A. calcd. for $C_{21}H_{22}F_3NO_3S$ (425,47): C, 59.28; H, 5.21; N, 3.29. Found: C, 59.13; H, 5.08; N, 3.38.

(R,S_S)**-*N-tert*-butanesulfinyl-1-(1,3-dioxocyclohexan-2-yl)-2,2,2-trifluoroethylamine [**(R,S_s)**-3e].** 2:1 Mixture of tautomeric forms *C* and *D*. Major:). (C,S,S_s)**-3e:** ^{1}H NMR δ 8.8 (bs, *1* H), 6.19 (d, *J* = 8.0 Hz, 1 H), 5.05 (quint, *J* = 8.0 Hz, 1 H), 2.4 (m, 4 H), 1.9 (m, 2 H), 1.14 (s, 9 H); ^{13}C NMR δ 192.5, 183.3, 125.4 (q, *J* = 283 Hz), 107.5, 57.5, 54.4 (q, *J* = 33 Hz), 22.6, 20.8; ^{19}F NMR δ –72.72 (d, *J* = 7.3 Hz, 3 F). (D,S,S_s)**-3e:** ^{1}H NMR δ 8.8 (bs, *1* H), 6.52 (d, *J* = 8.7 Hz, 1 H), 5.05 (quint, *J* = 8.0 Hz, 1 H), 2.4 (m, 4 H), 1.9 (m, 2 H), 1.24 (s, 9 H); ^{13}C NMR δ 192.5, 183.3, 125.3 (q, *J* = 283 Hz), 107.6, 57.4, 55.0(q, *J* = 33 Hz), 22.9, 20.7; ^{19}F NMR δ –73.29 (d, *J* = 7.3 Hz, 3 F). HRMS: calcd, 313,0959. HRMS: calcd, 313,0959. Found, 313.0950.

General procedure for the of DBU catalyzed addition of dicarbonyl compounds ***2a-e*** *to* (S_S)*-N-tert-butanesulfinyltrifluoroacetaldimine in dichloromethane at –10 °C.*

1,5-Diazabiciclo[5,4,0]undec-7-ene (DBU) (0.1 eq) was added to a solution of (*S*)-*N*-tert-butanesulfinyl-3,3,3-trifluoroacetaldimine (0.62 g, 3.0 mmol) and 1,3-dicarbonylcompound (1.1 eq) in dichloromethane (10 mL) at –10 °C, under nitrogen atmosphere. The mixture was allowed to react 4 h at this temperature before HCl (4N, 1 mL) was added while stirring. The organic phase was then washed with sat. $NaHCO_3$ (30 mL) and dried with Na_2SO_4. After solvent evaporation, a portion of the crude product was analyzed by ^{19}F NMR in order to determine the diastereomeric ratio (dr). Chromatography of the crude on silica gel (eluent CH_2Cl_2/EtOAc 60:40) allowed to recover the reaction product which was characterized as follows.

(S,S_s)**-2-Acetyl-*N*-(*tert*-butanesulfinyl)-3-oxo-1-(trifluoromethyl)butylamine** **[**(S,S_s)**-3a]**. White crystals, m.p. 130–132 °C; ^{1}H NMR δ 4.54 (quint, *J* = 7.6 Hz, 1 H), 4.39 (d, *J* = 9.2 Hz, 1 H), 4.35 (d, *J* = 8.0 Hz, 1 H), 2.32 (s, 3 H), 2.30 (s, 3 H), 1.20 (s, 9 H). ^{13}C NMR δ 201.1, 199.3, 124.9 (q, *J* = 281 Hz), 66.1, 57.8 (q, *J* = 30 Hz), 57.7, 31.6, 30.4, 22.7 (3 C). ^{19}F NMR δ –71.85 (d, *J* = 7.4 Hz, 3 F). Elem. A. calcd. for C, 43.85; H, 6.02; N, 4.65. Found: C, 43.71; H, 5.91; N, 4.73.

Methyl (S,S_s)-2-acetyl-3-amino-*N*-(*tert*-butanesulfinyl)-4,4,4-trifluorobutyrate [(S,S_s)-3b]. Mixture of epimers at the dicarbonyl α-carbon (A/B = 0.9). (A,S,S_s)-**3b**: white solid m.p. 125–128 °C; ^{1}H NMR δ 4.82 (d, *J* = 9.6 Hz, 1 H), 4.49 (m, 1 H), 4.15 (d, *J* = 5.9 Hz, 1 H), 3.79 (s, 3 H), , 2.36 (s, 3 H), 1.21 (s, 9 H); ^{13}C NMR δ 201.4, 166.7, 124.7 (q, *J* = 282 Hz), 58.7 (q, *J* = 31 Hz), 57.5, 53.7, 32.1, 22.7 (3 C); ^{19}F NMR δ –72.45 (d, *J* = 7.9 Hz, 3 F). (B,S,S_s)-**3b:** ^{1}H NMR δ 4.75 (d, *J* = 10 Hz, 1 H), 4.4 (m, 1 H), 3.87 (d, *J* = 4.9 Hz, 1 H), 3.74 (s, 3 H), 2.25 (s, 3 H), 1.19 (s, 9 H); ^{13}C NMR δ 198.1, 168.4, 124.7 (q, *J* = 282 Hz), 58.6 (q, *J* = 31 Hz), 57.8, 56.3, 29.5, 22.8 (3 C); ^{19}F NMR δ –73.61 (d, *J* = 7.8 Hz, 3 F). Elem. A. calcd. for $C_{11}H_{18}F_3NO_4S$ (317,32): C, 41.64; H, 5.72; N, 4.41. Found: C, 41.59; H, 5.65; N, 4.39.

(S,S_s)-2-Acetyl-*N*-(*tert*-butanesulfinyl)-3-oxo-3-phenyl-1-(trifluoromethyl)propylamine (S,S_s)-(3c). Viscous oil, mixture of two epimers at the dicarbonyl α-carbon (A/B = 1.0). (A,S,S_s)-**3c**: ^{1}H NMR δ 7.97 (d, *J* = 7.5 Hz, 2 H), 7.64 (t, *J* = 7.5 Hz, 1 H), 7.52 (t, *J* = 7.6 Hz, 2 H), 5.08 (d, *J* = 6.7 Hz, 1 H), 4.77 (quint.d, *J* = 7.7 and 2.4 Hz, 1 H), 4.56 (d, *J* = 10 Hz, 1 H), 2.18 (s, 3 H), 1.11 (s, 9 H); ^{13}C NMR δ 198.9, 192.3, 136.7, 135.1, 129.7, 129.7, 129.1, 124.9 (q, *J* = 282 Hz), 59.7, 58.4 (q, *J* = 30 Hz), 57.7, 30.7, 22.8; ^{19}F NMR δ –71.43 (d, *J* = 7.3 Hz, 3 F). (B,S,S_s)-**3c.** ^{1}H NMR δ 7.99 (d, *J* = 7.8 Hz, 2 H), 7.66 (t, *J* = 7.4 Hz, 1 H), 7.54 (t, *J* = 7.8 Hz, 2 H), 5.26 (d, *J* = 8.5 Hz, 1 H), 4.71 (sext, *J* = 8.0 Hz, 1 H), 4.61 (d, *J* = 9.3 Hz, 1 H), 2.19 (s, 3 H), 1.18 (s, 9 H); ^{13}C NMR δ 199.9, 194.3, 135.6, 135.1, 129.7, 129.2, 125.1 (d, *J* = 282 Hz), 60.8, 58.6 (q, *J* = 30 Hz), 57.8, 29.8, 22.7; ^{19}F NMR δ –72.43 (d, *J* = 7.5 Hz, 3 F). HRMS, calcd for $C_{16}H_{20}F_3NO_3S$ (363,1116). Found, 363.1120.

(R,S_s)-2-Acetyl-*N*-(*tert*-butanesulfinyl)-3-oxo-3-phenyl-1-(trifluoromethyl)-propylamine [(R,$\mathrm{S_s}$)-3c]. 1.5:1 mixture of two epimers (*A*,*B*) at the dicarbonyl α-carbon (*A*/*B* = 1.5): (A,R,S_s)-**3c**: white solid, m.p. 125–127 °C; ^{1}H NMR δ 7.96 (d, *J* = 7.7 Hz, 2 H), 7.67 (t, *J* = 7.5 Hz, 1 H), 7.54 (t, *J* = 7.5 Hz, 2 H), 5.71 (d, *J* = 8.1 Hz, 1 H), 4.88 (d, *J* = 3.0 Hz, 1 H), 4.66 (quint.d, *J* = 8.0 and 3.0 Hz, 1 H), 2.25 (s, 3 H), 1.25 (s, 9 H); ^{13}C NMR δ 199.5, 197.8, 137.0, 135.2, 129.7, 129.0, 125.1 (q, *J* = 280 Hz), 59.7 (q, *J* = 31 Hz), 57.4, 56.9, 30.2, 22.8; ^{19}F NMR δ –74.31 (d, *J* = 7.8 Hz, 3 F). (B,R,S_s)-**3c.** ^{1}H NMR δ 7.98 (d, *J* = 7.5 Hz, 2 H), 7.65 (t, *J* = 7.5 Hz, 1 H), 7.52 (t, *J* = 7.4 Hz, 2 H), 4.95 (d, *J* = 6.4 Hz, 1 H), 4.52 (quint, *J* = 6.3 Hz, 1 H), 4.36 (d, *J* = 8.8 Hz, 1 H), 2.29 (s, 3 H), 1.23 (s, 9 H); ^{13}C NMR δ 202.7, 196.0, 136.5, 134.9, 129.7, 129.2, 124.8 (d, *J* = 281 Hz), 58.3 (q, *J* = 30 Hz), 57.5, 57.3, 30.2, 22.8; ^{19}F NMR δ –74.91 (d, *J* = 7.0 Hz, 3 F). Elem. A. calcd. for $C_{16}H_{20}F_3NO_3S$ (363,40) C, 52.88; H, 5.55; N, 3.85. Found, C, 52.83; H, 5.61; N, 3.92.

(R,S_s)- **and** (S,S_s)-**3-Benzoyl-*N*-(*tert*-butanesulfinyl)-3-oxo-3-phenyl-1-(trifluoromethyl)propyl-amine [(R,S_s)-3d** and (S,S_s)-**3d]**. Sticky solid, mixture of two diastereomers. (R,S_s)-**3d** (major): ^{1}H NMR δ 8.02 (d, *J* = 7.2 Hz, 4 H), 7.58 (t, *J* = 7.2 Hz, 2 H), 7.51 (t, *J* = 7.7 Hz, 4 H), 5.92 (d, *J* = 3.4 Hz, 1 H), 5.87 (d, *J* = 8.0 Hz, 1 H), 4.59 (quint.d, *J* = 8.0 and 3.4 Hz, 1 H), 1.24 (s, 9 H); ^{13}C NMR δ 194.9, 191.7, 136.6, 135.1, 134.8, 134.7, 129.7, 129.5, 129.2, 128.8, 125.0 (q, *J* = 280 Hz), 59.4 (q, *J* = 30 Hz), 57.4, 52.2, 22.8; ^{19}F

NMR δ –74.05 (d, *J* = 7.7 Hz, 3 F). (*S*,*S*$_s$)**-3d** (minor): ^{1}H NMR δ 7.95 (d, *J* = 7.5 Hz, 4 H), 7.65 (t, *J* = 7.4 Hz, 1 H), 7.60 (t, *J* = 7.4 Hz, 1 H), 7.52 (t, *J* = 7.7 Hz, 2 H), 7.47 (t, *J* = 7.7 Hz, 2 H), 5.95 (d, *J* = 6.6 Hz, 1 H), 4.89 (quint.d, *J* = 7.3 and 2.6 Hz, 1 H), 4.72 (d, *J* = 10 Hz, 1 H), 1.09 (s, 9 H); ^{13}C NMR δ 192.9, 191.8, 136.4, 135.1, 134.8, 134.7, 129.7, 129.6, 129.00, 128.9, 125.1 (q, *J* = 283 Hz), 59.4 (q, *J* = 30 Hz), 57.8, 54.0, 22.6; ^{19}F NMR δ –72.26 (d, *J* = 7.4 Hz, 3 F). Elem. A. calcd. for $C_{21}H_{22}F_3NO_3S$ (425,47) C, 59.28; H, 5.21; N, 3.29. Found C, 59.11; H, 5.06; N, 3.18.

(*S*,*S*$_s$)**-*N-tert*-butanesulfinyl-1-(1,3-dioxocyclohexan-2-yl)-2,2,2-trifluoroethylamine [**(*S*,*S*$_s$)**-3e].** Mixture of two tautomeric forms (*C*/*D* = 2). (*C*,*S*,*S*$_s$)**-3e:** ^{1}H NMR δ 8.8 (bs, *1* H), 6.19 (d, *J* = 8.0 Hz, 1 H), 5.05 (quint, *J* = 8.0 Hz, 1 H), 2.4 (m, 4 H), 1.9 (m, 2 H), 1.14 (s, 9 H); ^{13}C NMR δ 192.5, 183.3, 125.4 (q, *J* = 283 Hz), 107.5, 57.5, 54.4 (q, *J* = 33 Hz), 22.6, 20.8; ^{19}F NMR δ –72.72 (d, *J* = 7.3 Hz, 3 F). (*D*,*S*,*S*$_s$)**-3e**: ^{1}H NMR δ 8.8 (bs, *1* H), 6.52 (d, *J* = 8.7 Hz, 1 H), 5.05 (quint, *J* = 8.0 Hz, 1 H), 2.4 (m, 4 H), 1.9 (m, 2 H), 1.24 (s, 9 H); ^{13}C NMR δ 192.5, 183.3, 125.3 (q, *J* = 283 Hz), 107.6, 57.4, 55.0(q, *J* = 33 Hz), 22.9, 20.7; ^{19}F NMR δ –73.29 (d, *J* = 7.3 Hz, 3 F). HRMS: calcd, 313,0959. HRMS, calcd for $C_{12}H_{18}F_3NO_3S$ (313,0959). Found, 3130960.

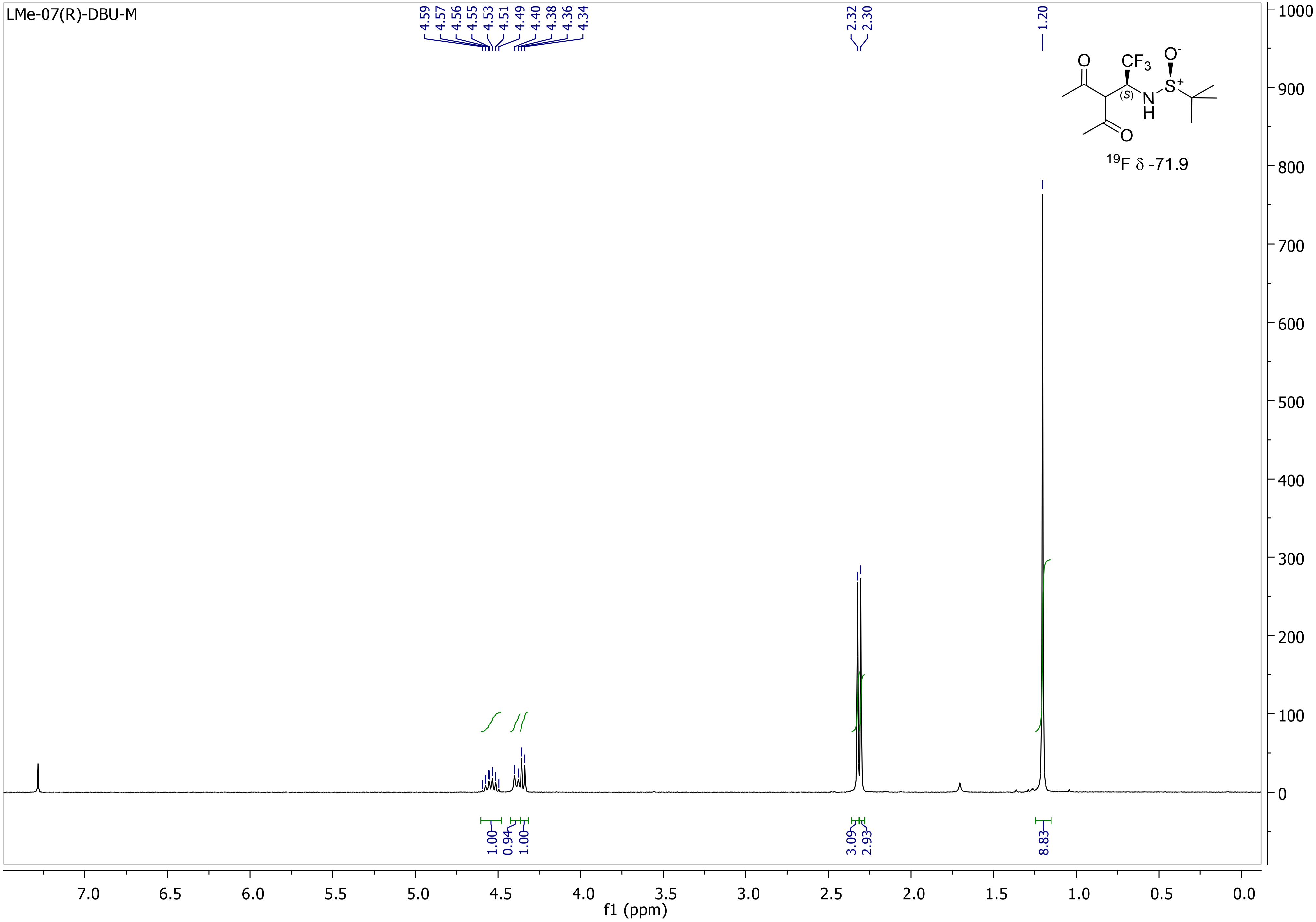
LMe-07(R)-DBU-M
4.59
4.57
4.56
4.55
4.53
4.51
4.49
4.40
4.38
4.36
4.34
2.32
2.30
1.20
O
CF$_3$
O$^-$
S$^+$
(S)
N
H
O
^{19}F δ -71.9
1.00
0.94
1.00
3.09
2.93
8.83
7.0
6.5
6.0
5.5
5.0
4.5
4.0
3.5
3.0
2.5
2.0
1.5
1.0
0.5
0.0
f1 (ppm)
1000
900
800
700
600
500
400
300
200
100
0

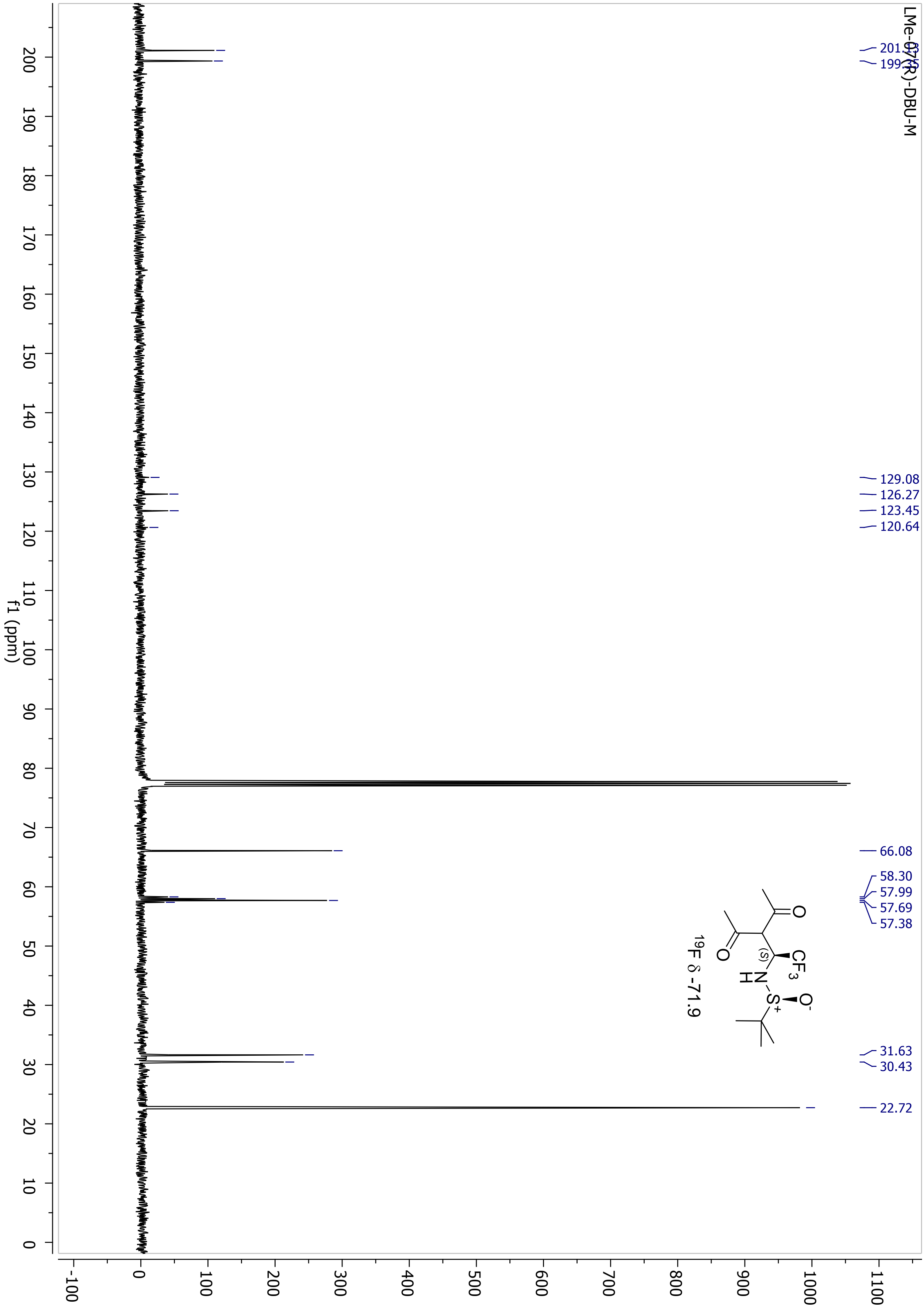
LMe-07(R)-DBU-M
201.13
199.35
129.08
126.27
123.45
120.64
66.08
58.30
57.99
57.69
57.38
31.63
30.43
22.72
O
O
CF3
(S)
N
H
S+
O-
19F δ -71.9
f1 (ppm)
200
190
180
170
160
150
140
130
120
110
100
90
80
70
60
50
40
30
20
10
0
-100
0
100
200
300
400
500
600
700
800
900
1000
1100

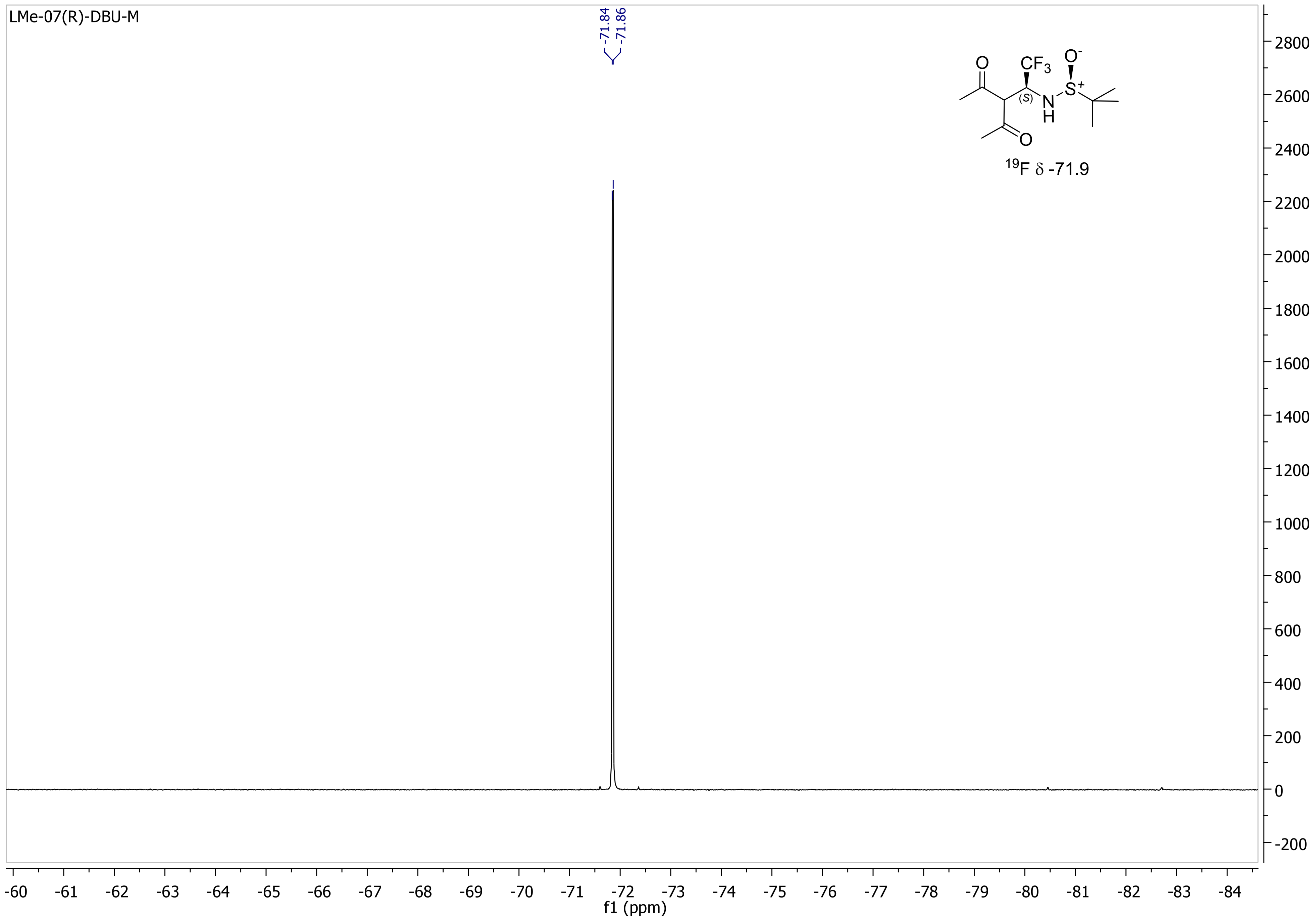
LMe-07(R)-DBU-M
-71.84
-71.86
O
CF3
O-
(S)
N
H
S+
O
19F δ -71.9
-60 -61 -62 -63 -64 -65 -66 -67 -68 -69 -70 -71 -72 -73 -74 -75 -76 -77 -78 -79 -80 -81 -82 -83 -84
f1 (ppm)
2800 2600 2400 2200 2000 1800 1600 1400 1200 1000 800 600 400 200 0 -200

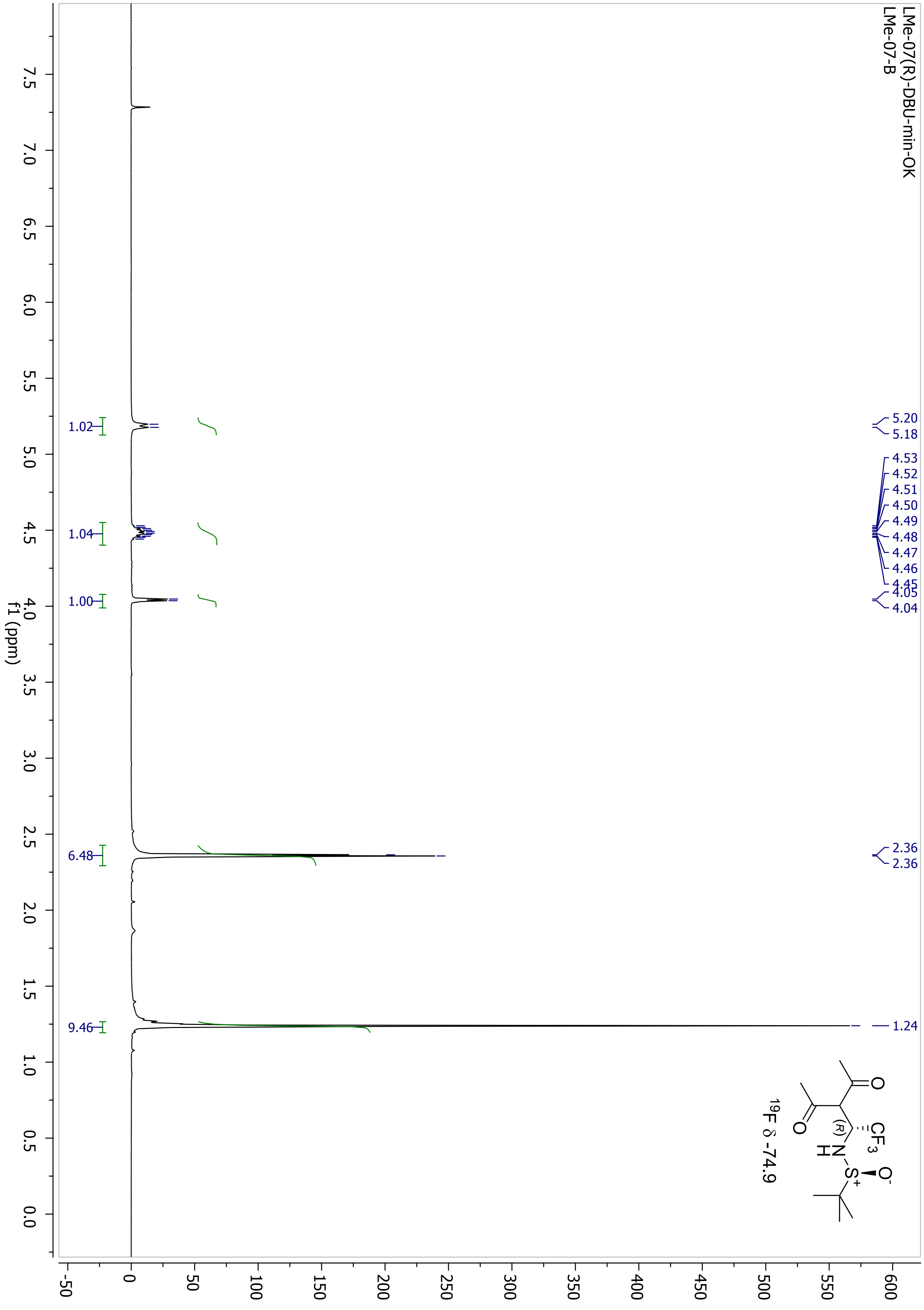
LMe-07(R)-DBU-min-OK
LMe-07-B
5.20
5.18
4.53
4.52
4.51
4.50
4.49
4.48
4.47
4.46
4.45
4.05
4.04
2.36
2.36
1.24
1.02
1.04
1.00
6.48
9.46
7.5
7.0
6.5
6.0
5.5
5.0
4.5
4.0
3.5
3.0
2.5
2.0
1.5
1.0
0.5
0.0
f1 (ppm)
-50
0
50
100
150
200
250
300
350
400
450
500
550
600
O
O
CF3
O-
(R)
N
H
S+
19F δ -74.9

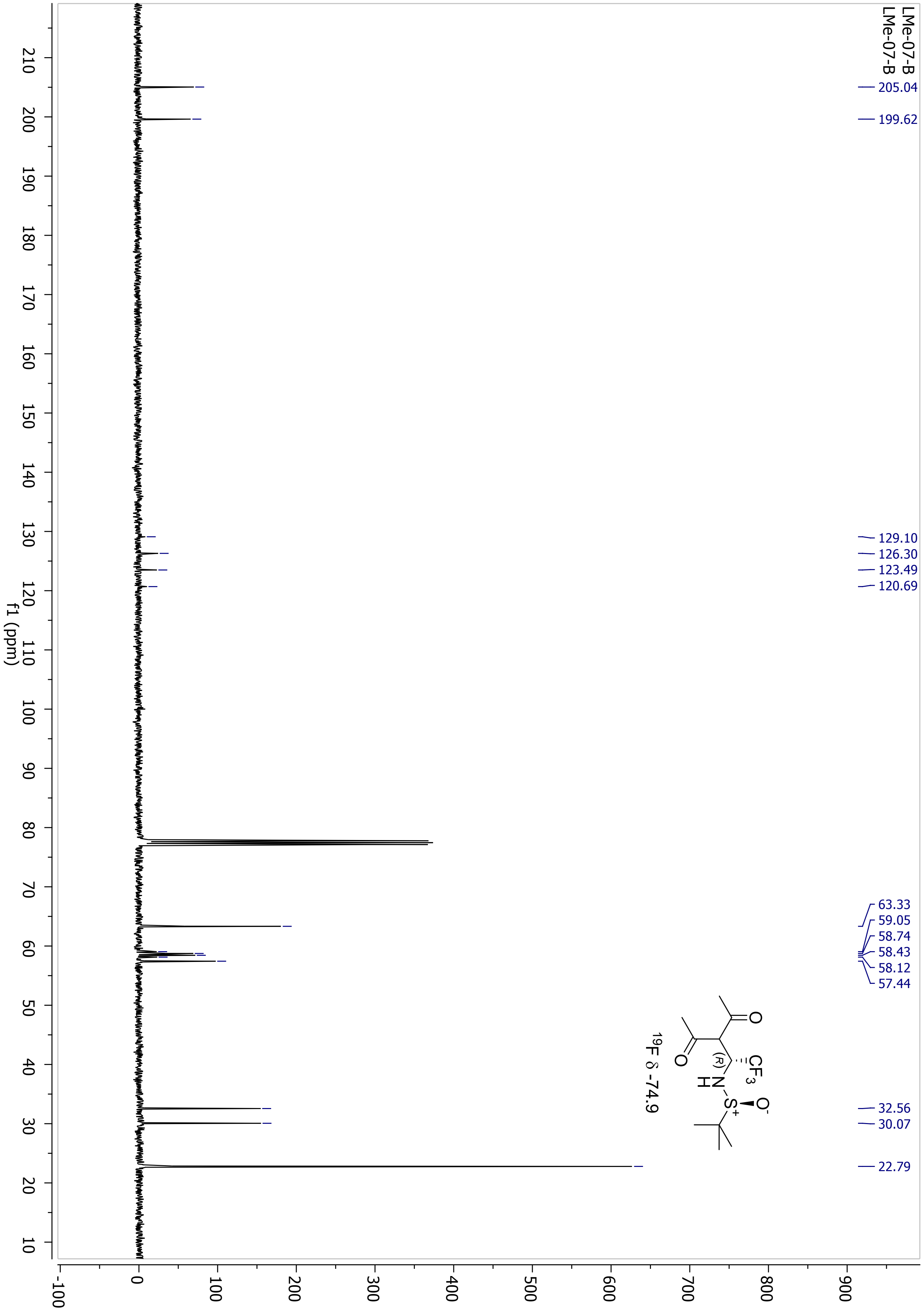
LMe-07-B
LMe-07-B
205.04
199.62
129.10
126.30
123.49
120.69
63.33
59.05
58.74
58.43
58.12
57.44
32.56
30.07
22.79
O
O
CF3
(R)
N
H
S+
O-
19F δ -74.9
f1 (ppm)
210
200
190
180
170
160
150
140
130
120
110
100
90
80
70
60
50
40
30
20
10
-100
0
100
200
300
400
500
600
700
800
900

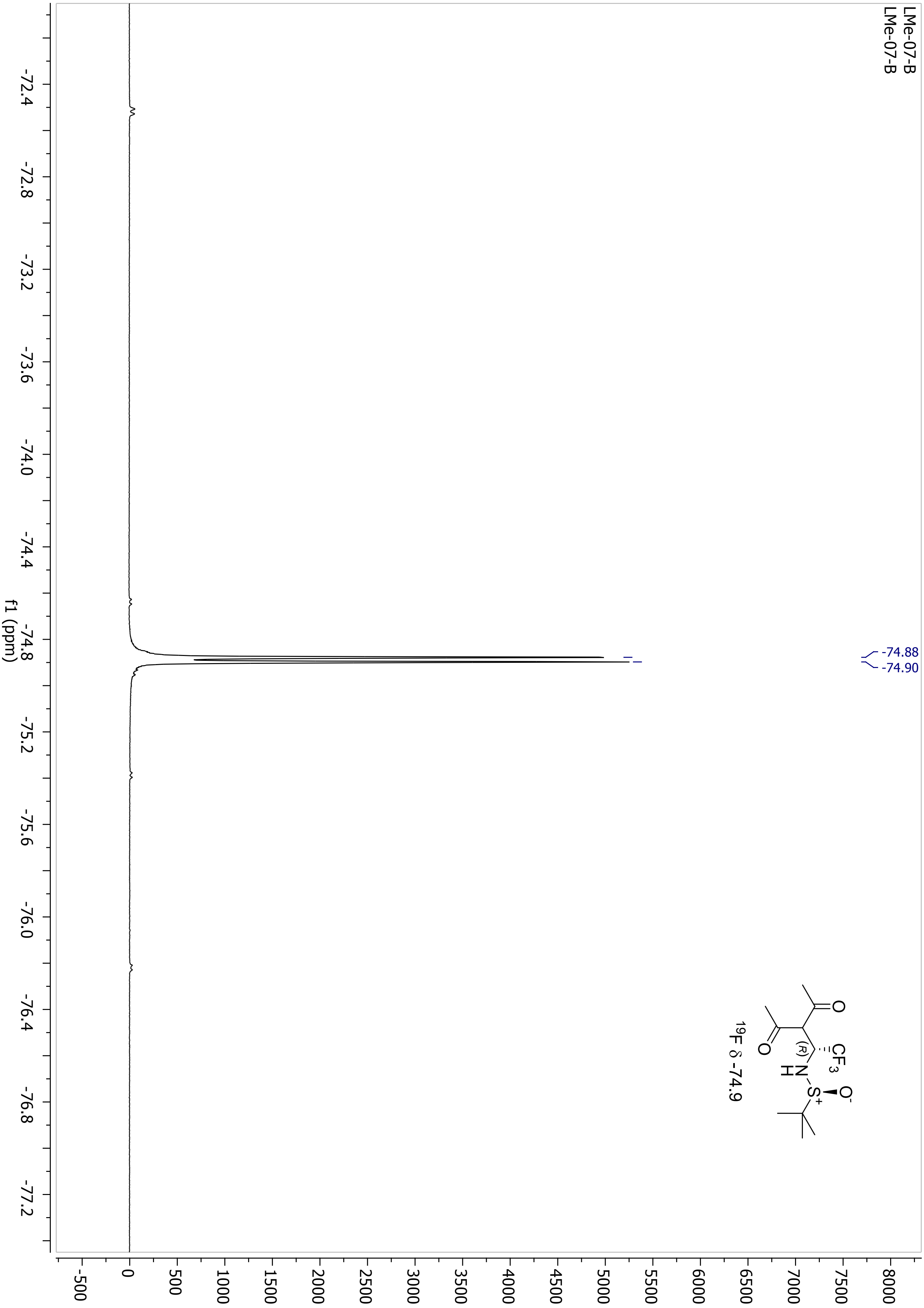
LMe-07-B
LMe-07-B
-74.88
-74.90
CF$_3$
O$^-$
S$^+$
N
H
(R)
O
O
^{19}F δ -74.9
-72.4
-72.8
-73.2
-73.6
-74.0
-74.4
-74.8
-75.2
-75.6
-76.0
-76.4
-76.8
-77.2
f1 (ppm)
-500
0
500
1000
1500
2000
2500
3000
3500
4000
4500
5000
5500
6000
6500
7000
7500
8000

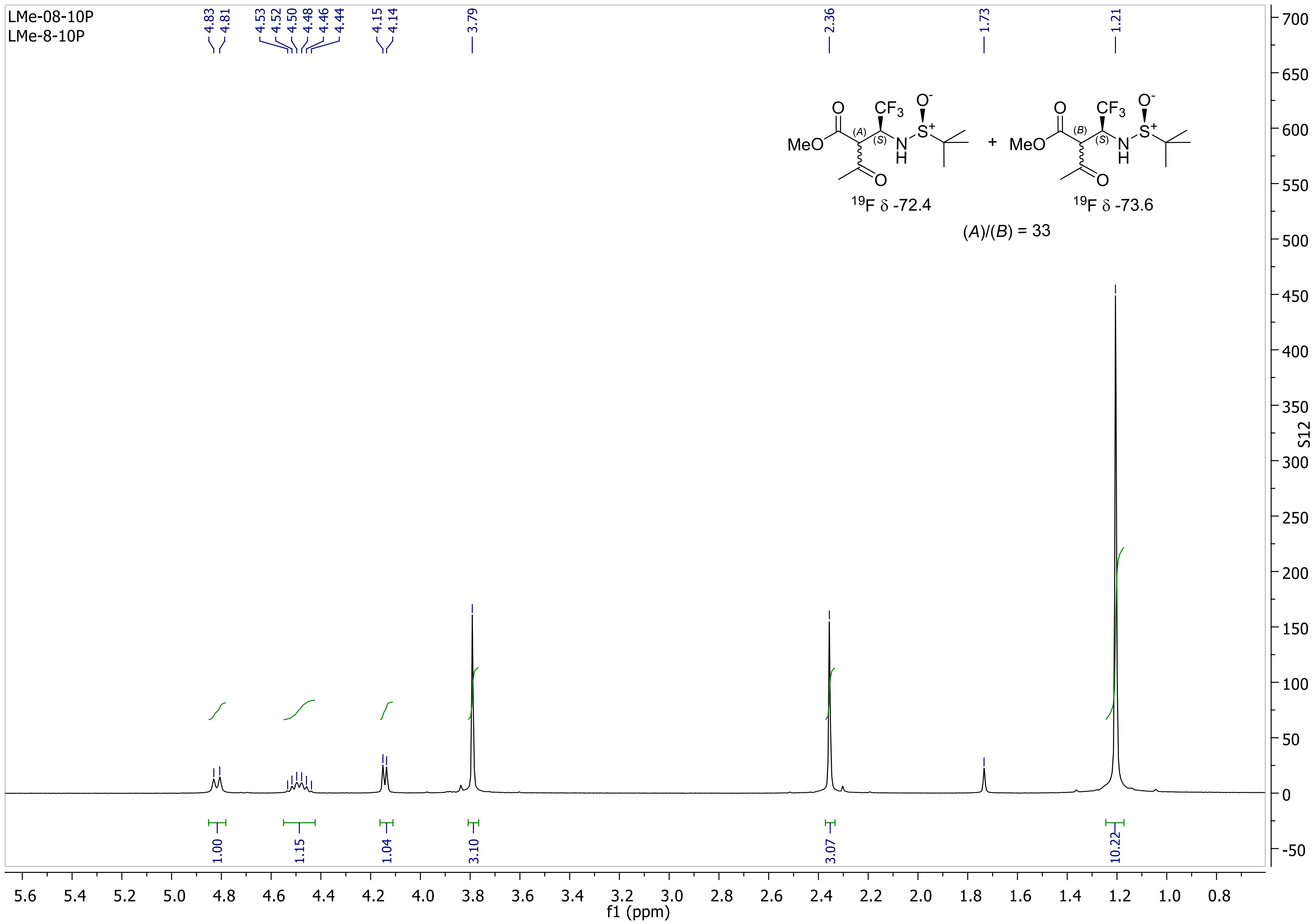
LMe-08-10P
LMe-8-10P
4.83
4.81
4.53
4.52
4.50
4.48
4.46
4.44
4.15
4.14
3.79
2.36
1.73
1.21
MeO
O
CF3
O-
S+
N
H
(A)
(S)
O
+
MeO
O
CF3
O-
S+
N
H
(B)
(S)
O
19F δ -72.4
19F δ -73.6
(A)/(B) = 33
1.00
1.15
1.04
3.10
3.07
10.22
5.6
5.4
5.2
5.0
4.8
4.6
4.4
4.2
4.0
3.8
3.6
3.4
3.2
3.0
2.8
2.6
2.4
2.2
2.0
1.8
1.6
1.4
1.2
1.0
0.8
f1 (ppm)
700
650
600
550
500
450
400
350
300
250
200
150
100
50
0
-50

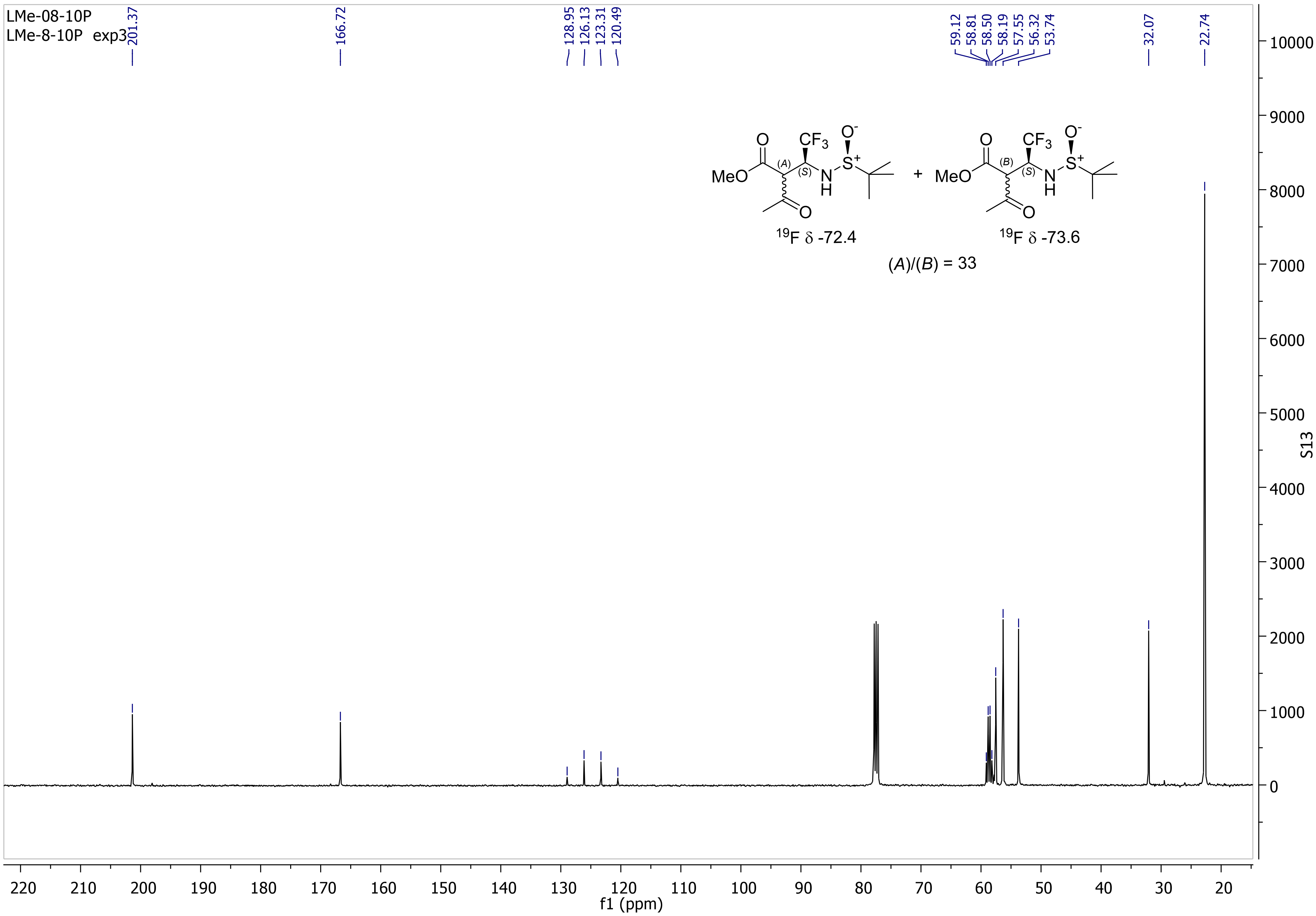
LMe-08-10P
LMe-8-10P exp3
201.37
166.72
128.95
126.13
123.31
120.49
59.12
58.81
58.50
58.19
57.55
56.32
53.74
32.07
22.74
MeO
O
(A)
(S)
CF3
N
H
S+
O-
O
19F δ -72.4
+
MeO
O
(B)
(S)
CF3
N
H
S+
O-
O
19F δ -73.6
(A)/(B) = 33
220
210
200
190
180
170
160
150
140
130
120
110
100
90
80
70
60
50
40
30
20
f1 (ppm)
10000
9000
8000
7000
6000
5000
4000
3000
2000
1000
0

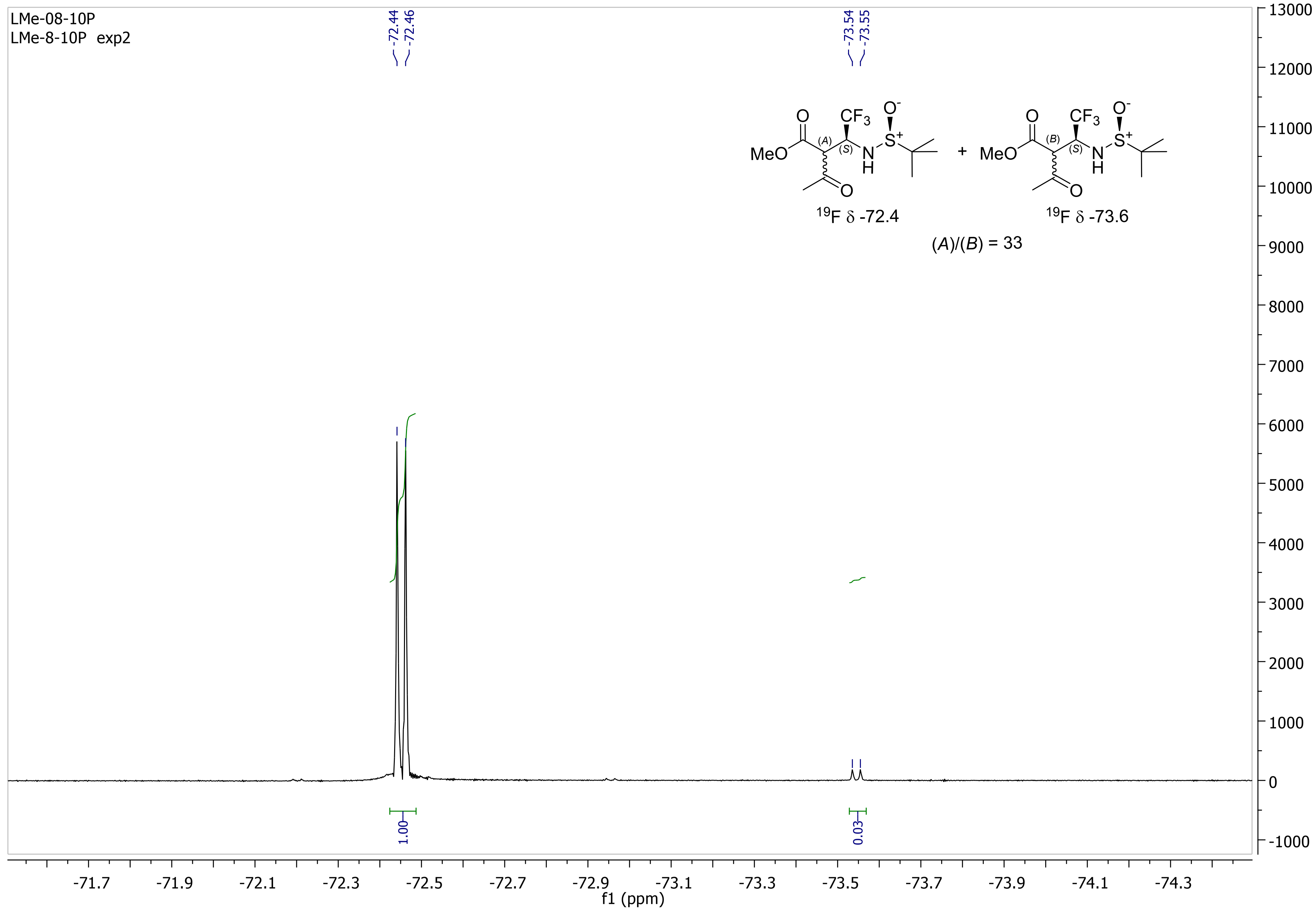
LMe-08-10P
LMe-8-10P exp2
-72.44
-72.46
-73.54
-73.55
MeO
O
CF3
O-
S+
N
H
(A)
(S)
+
(B)
19F δ -72.4
19F δ -73.6
(A)/(B) = 33
1.00
0.03
-71.7
-71.9
-72.1
-72.3
-72.5
-72.7
-72.9
-73.1
-73.3
-73.5
-73.7
-73.9
-74.1
-74.3
f1 (ppm)
13000
12000
11000
10000
9000
8000
7000
6000
5000
4000
3000
2000
1000
0
-1000

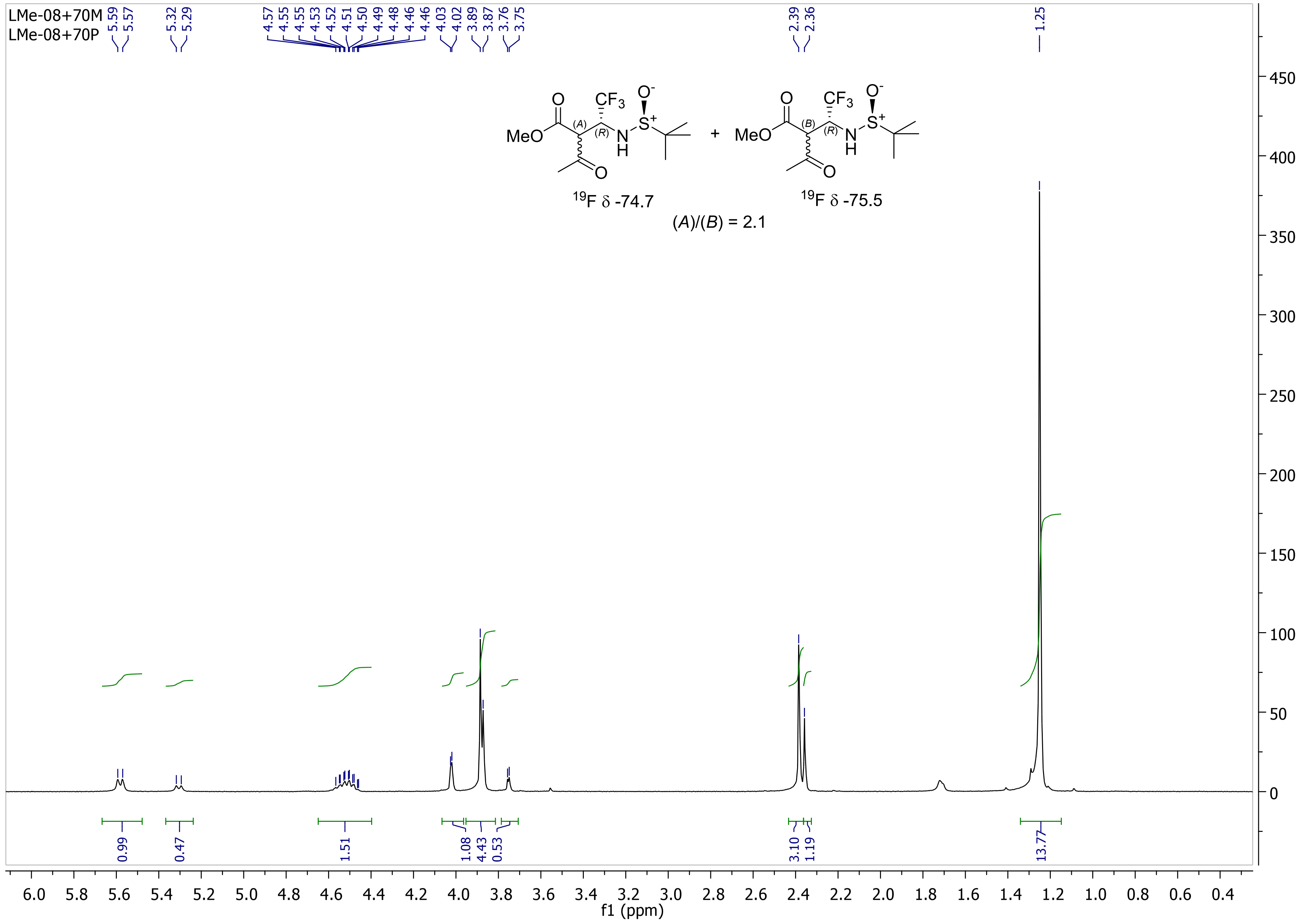
LMe-08+70M
LMe-08+70P
5.59
5.57
5.32
5.29
4.57
4.55
4.55
4.53
4.52
4.51
4.50
4.49
4.48
4.46
4.46
4.03
4.02
3.89
3.87
3.76
3.75
2.39
2.36
1.25
MeO
O
CF3
O-
S+
(A)
(R)
N
H
O
+
(B)
19F δ -74.7
19F δ -75.5
(A)/(B) = 2.1
0.99
0.47
1.51
1.08
4.43
0.53
3.10
1.19
13.77
6.0
5.8
5.6
5.4
5.2
5.0
4.8
4.6
4.4
4.2
4.0
3.8
3.6
3.4
3.2
3.0
2.8
2.6
2.4
2.2
2.0
1.8
1.6
1.4
1.2
1.0
0.8
0.6
0.4
f1 (ppm)
450
400
350
300
250
200
150
100
50
0

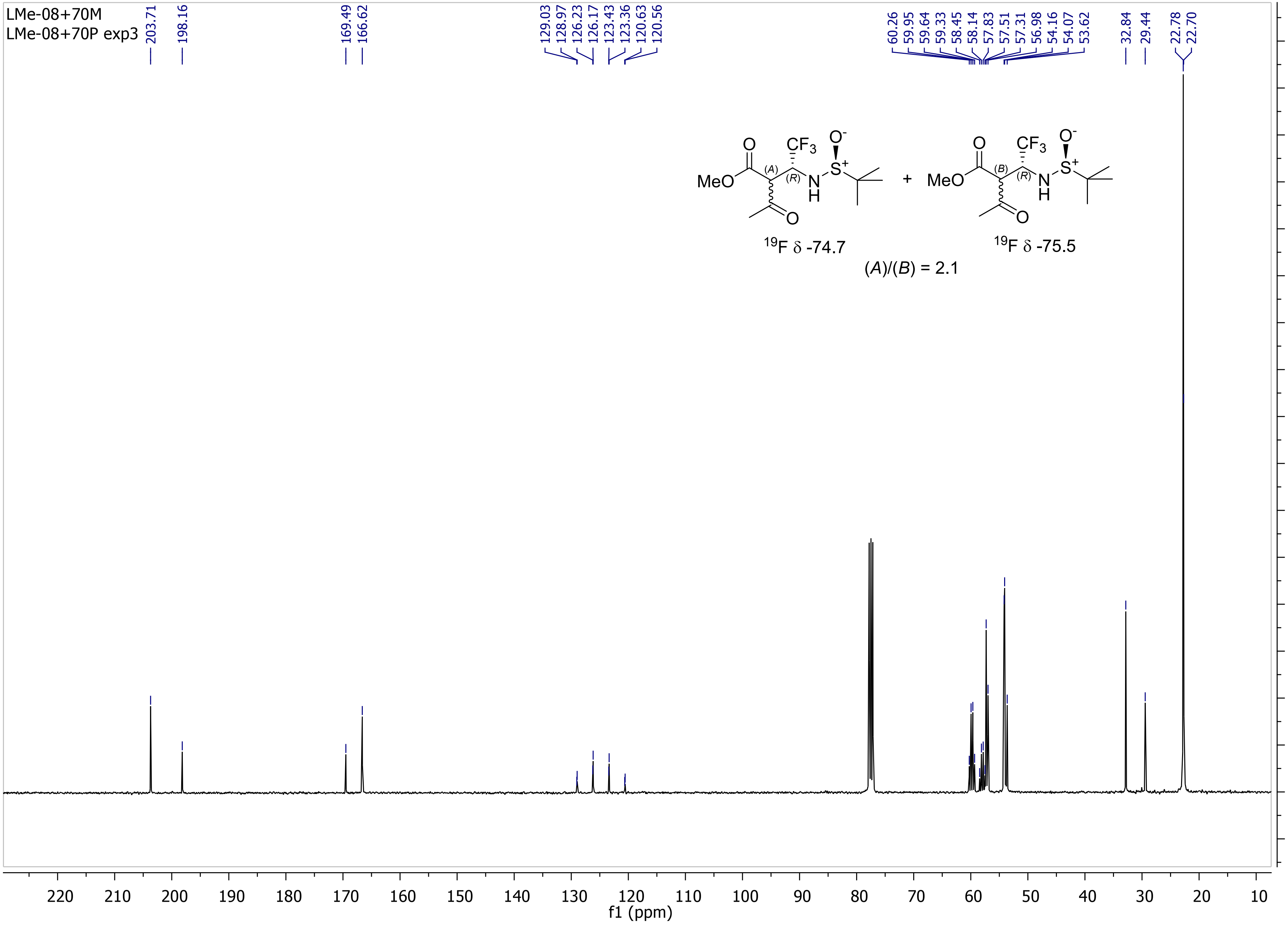
LMe-08+70M
LMe-08+70P exp3
203.71
198.16
169.49
166.62
129.03
128.97
126.23
126.17
123.43
123.36
120.63
120.56
60.26
59.95
59.64
59.33
58.45
58.14
57.83
57.51
57.31
56.98
54.16
54.07
53.62
32.84
29.44
22.78
22.70
MeO
O
(A)
(R)
CF3
N
H
S+
O-
O
+
(B)
19F δ -74.7
19F δ -75.5
(A)/(B) = 2.1
f1 (ppm)
220
210
200
190
180
170
160
150
140
130
120
110
100
90
80
70
60
50
40
30
20
10
8000
7500
7000
6500
6000
5500
5000
4500
4000
3500
3000
2500
2000
1500
1000
500
0
-500

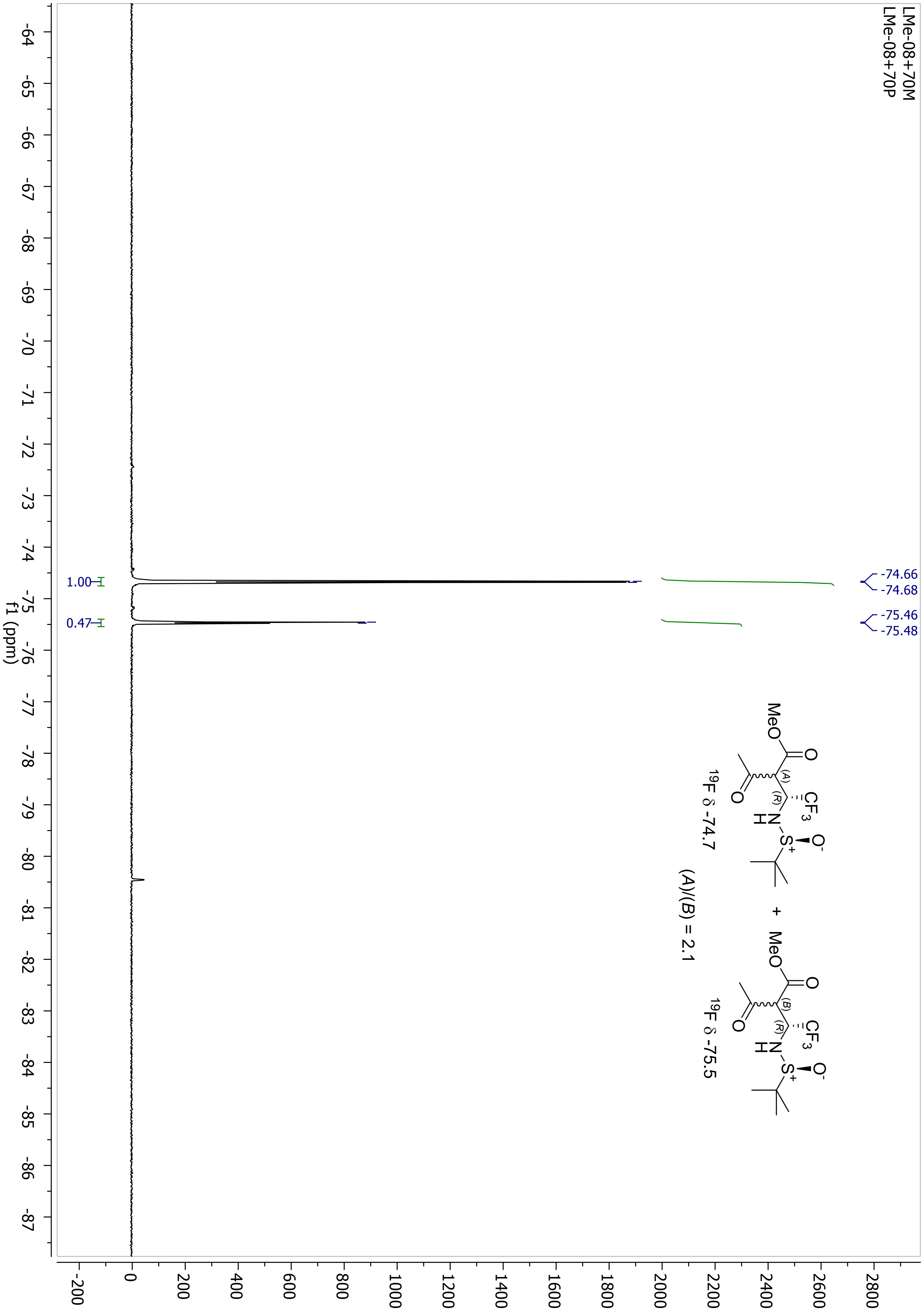
LMe-08+70M
LMe-08+70P
-74.66
-74.68
-75.46
-75.48
1.00
0.47
f1 (ppm)
MeO
O
CF3
O-
S+
N
H
(A)
(R)
(B)
19F δ -74.7
19F δ -75.5
(A)/(B) = 2.1
+

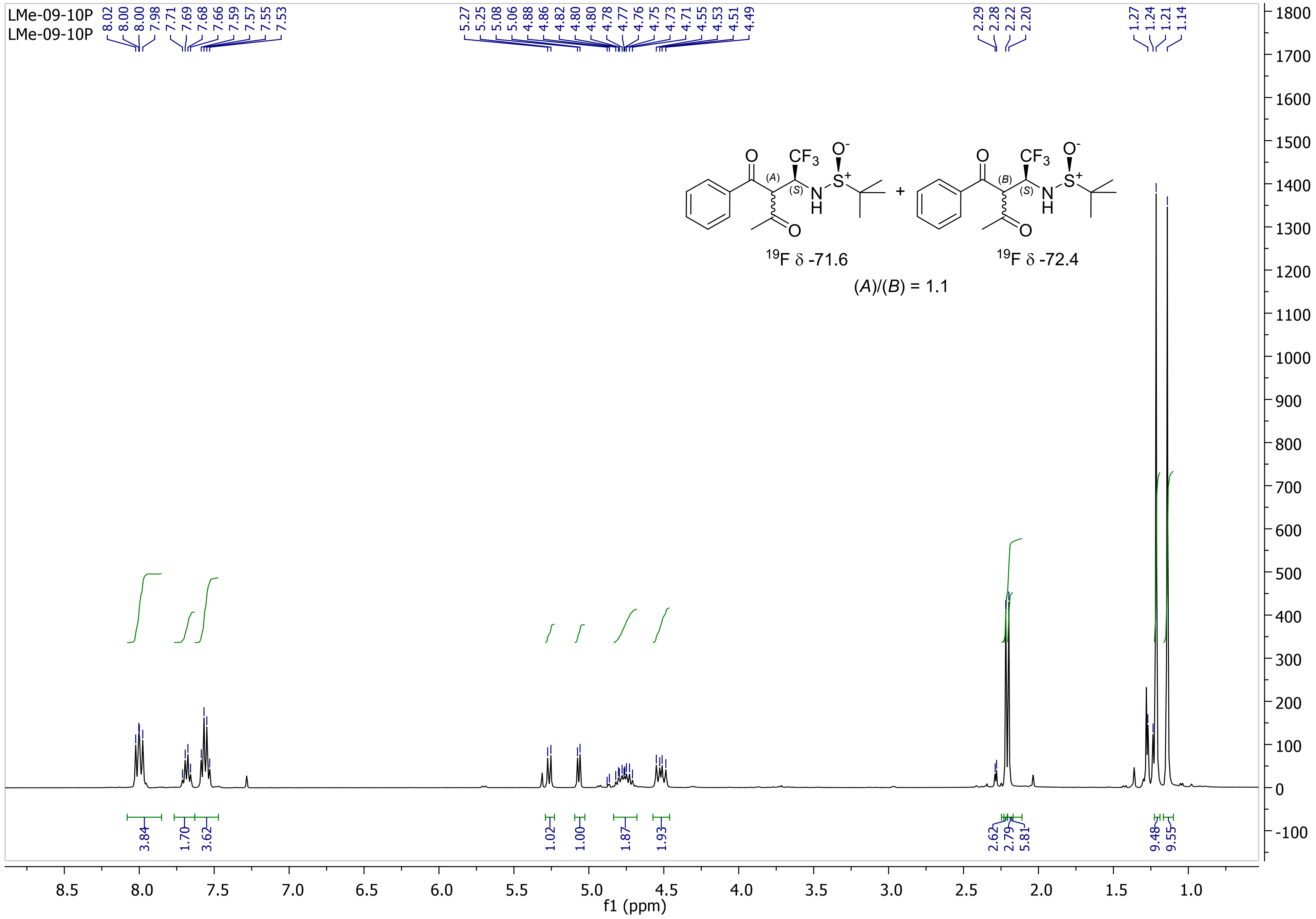
LMe-09-10P
LMe-09-10P
8.02
8.00
8.00
7.98
7.71
7.69
7.68
7.66
7.59
7.57
7.55
7.53
5.27
5.25
5.08
5.06
4.88
4.86
4.82
4.80
4.80
4.78
4.77
4.76
4.75
4.73
4.71
4.55
4.53
4.51
4.49
2.29
2.28
2.22
2.20
1.27
1.24
1.21
1.14
O
CF3
O-
S+
(A)
(S)
N
H
O
+
(B)
^{19}F δ -71.6
^{19}F δ -72.4
(A)/(B) = 1.1
3.84
1.70
3.62
1.02
1.00
1.87
1.93
2.62
2.79
5.81
9.48
9.55
8.5
8.0
7.5
7.0
6.5
6.0
5.5
5.0
4.5
4.0
3.5
3.0
2.5
2.0
1.5
1.0
f1 (ppm)
1800
1700
1600
1500
1400
1300
1200
1100
1000
900
800
700
600
500
400
300
200
100
0
-100

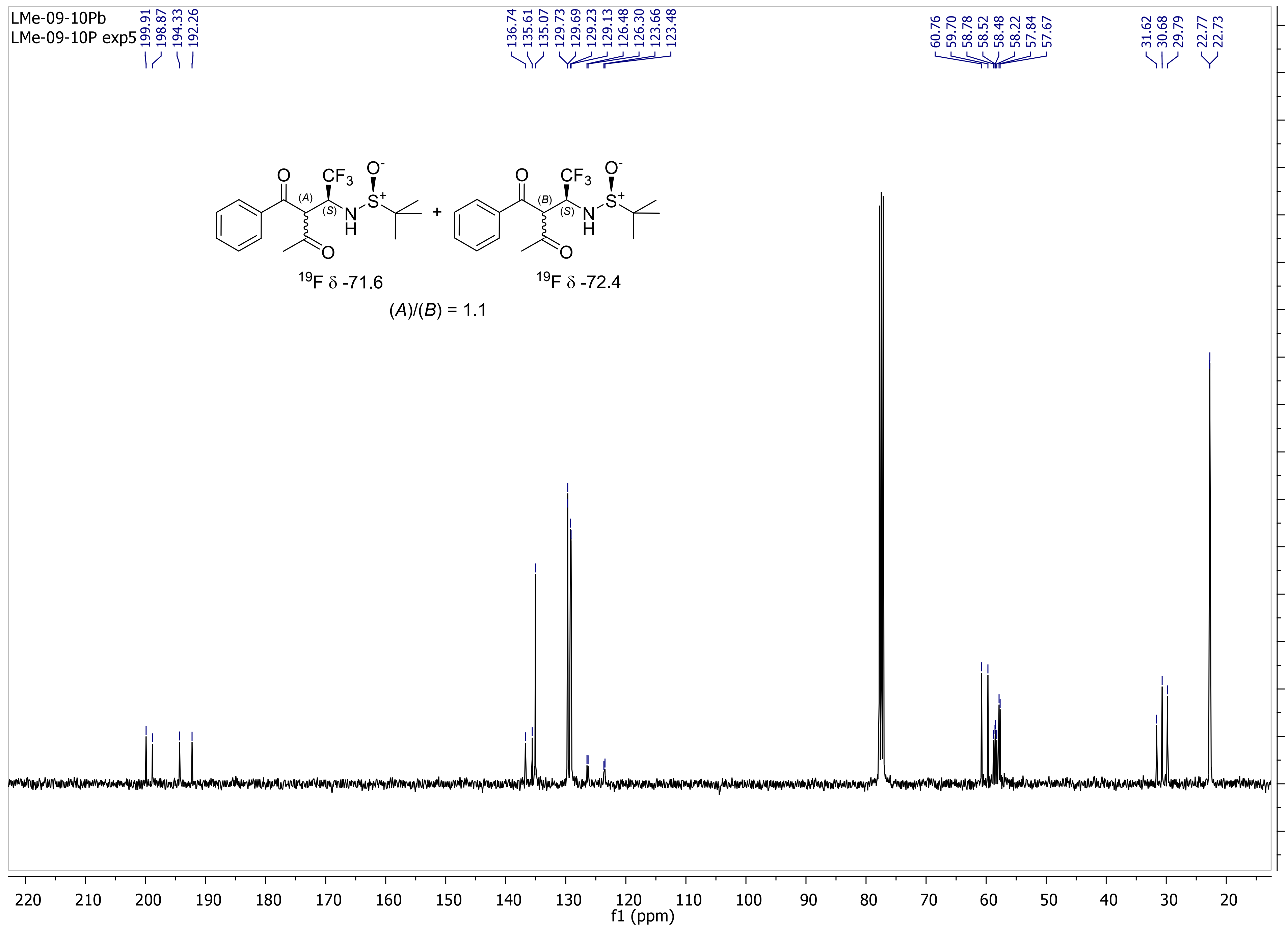
LMe-09-10Pb
LMe-09-10P exp5
199.91
198.87
194.33
192.26
136.74
135.61
135.07
129.73
129.69
129.23
129.13
126.48
126.30
123.66
123.48
60.76
59.70
58.78
58.52
58.48
58.22
57.84
57.67
31.62
30.68
29.79
22.77
22.73
O
CF3
O-
S+
(A)
(S)
N
H
O
+
(B)
^{19}F δ -71.6
^{19}F δ -72.4
(A)/(B) = 1.1
220
210
200
190
180
170
160
150
140
130
120
110
100
90
80
70
60
50
40
30
20
f1 (ppm)
800
750
700
650
600
550
500
450
400
350
300
250
200
150
100
50
0
-50

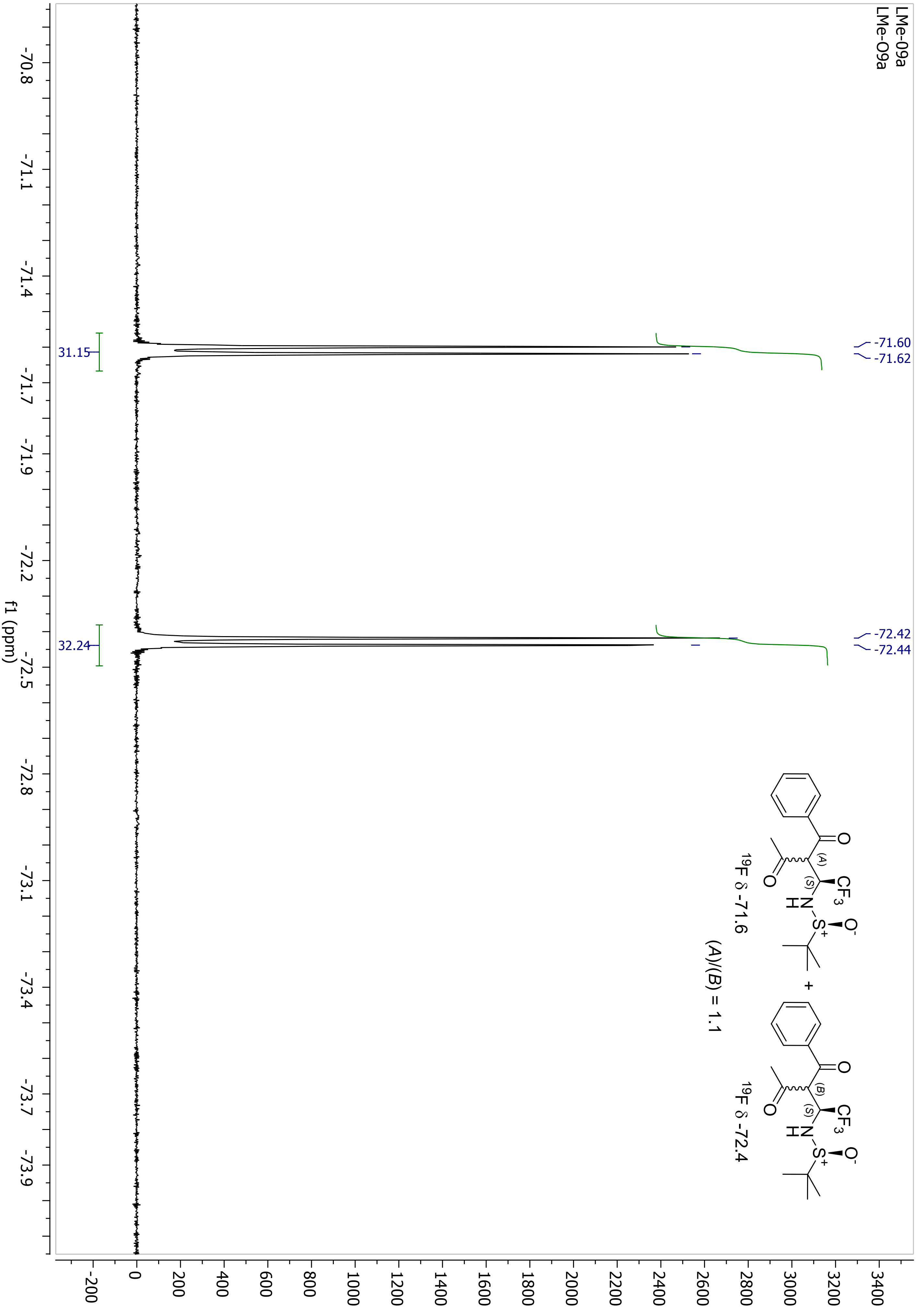
LMe-09a
LMe-O9a
-71.60
-71.62
-72.42
-72.44
31.15
32.24
-70.8
-71.1
-71.4
-71.7
-71.9
-72.2
-72.5
-72.8
-73.1
-73.4
-73.7
-73.9
f1 (ppm)
-200
0
200
400
600
800
1000
1200
1400
1600
1800
2000
2200
2400
2600
2800
3000
3200
3400
(A)
(S)
(B)
^{19}F δ -71.6
^{19}F δ -72.4
(A)/(B) = 1.1

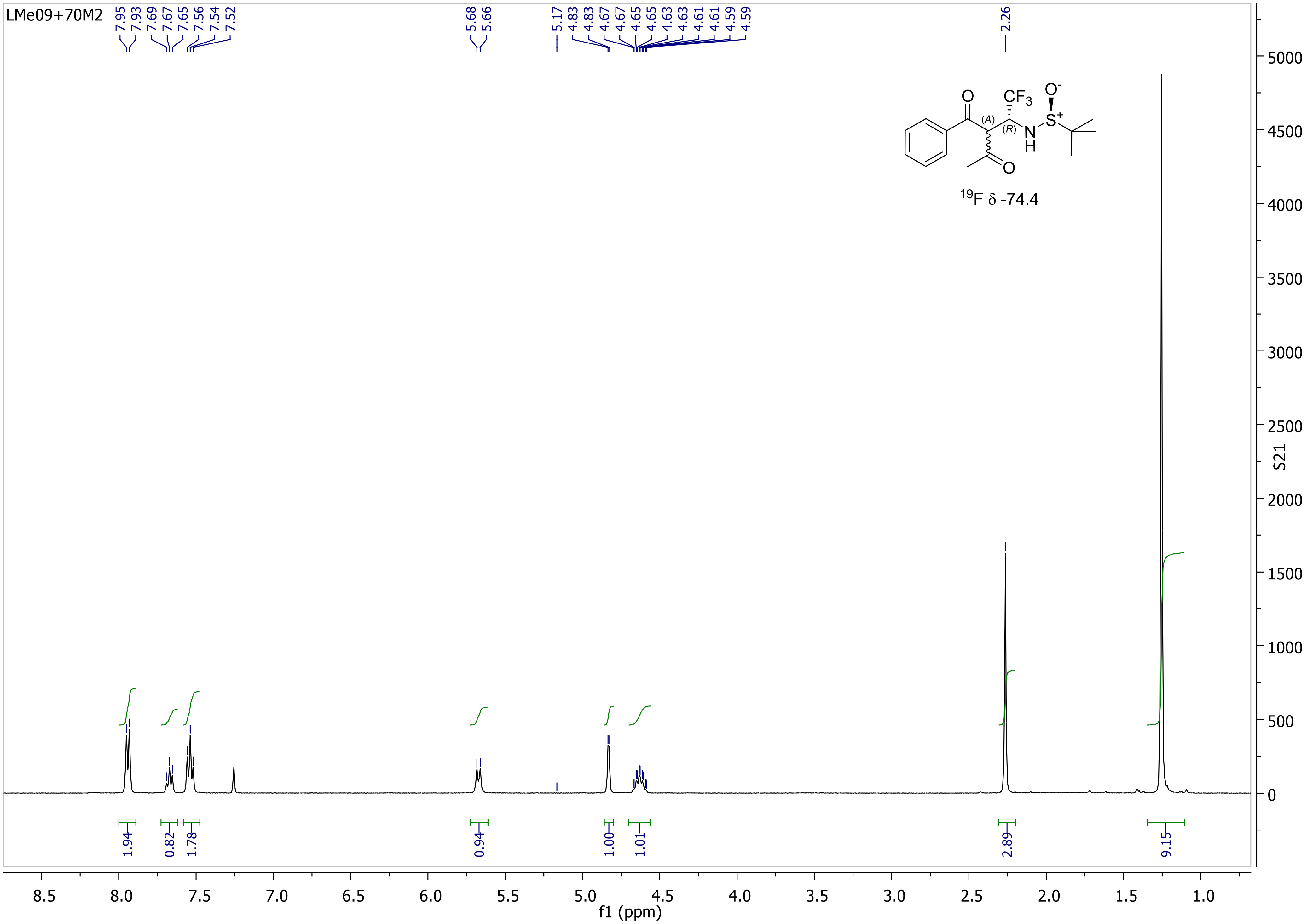
LMe09+70M2
7.95
7.93
7.69
7.67
7.65
7.56
7.54
7.52
5.68
5.66
5.17
4.83
4.83
4.67
4.67
4.65
4.65
4.63
4.63
4.61
4.61
4.59
4.59
2.26
O
CF3
O-
(A)
(R)
N
H
S+
O
1.94
0.82
1.78
0.94
1.00
1.01
2.89
9.15
8.5
8.0
7.5
7.0
6.5
6.0
5.5
5.0
4.5
4.0
3.5
3.0
2.5
2.0
1.5
1.0
f1 (ppm)
5000
4500
4000
3500
3000
2500
2000
1500
1000
500
0

^{19}F δ -74.4

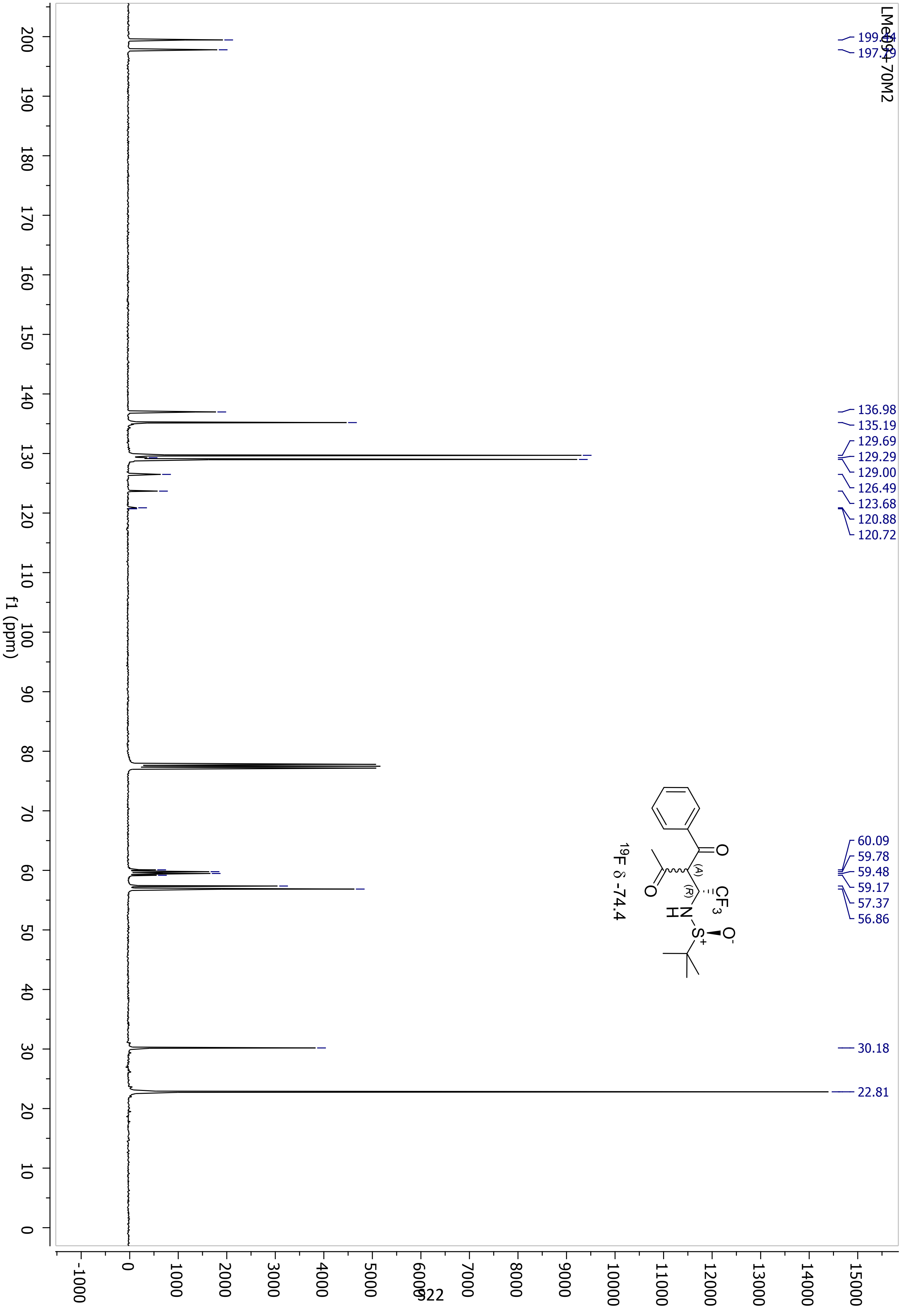
LMe09-70M2
199.44
197.79
136.98
135.19
129.69
129.29
129.00
126.49
123.68
120.88
120.72
60.09
59.78
59.48
59.17
57.37
56.86
30.18
22.81
O
CF3
(A)
(R)
O
N
H
S+
O-
19F δ -74.4
f1 (ppm)
200
190
180
170
160
150
140
130
120
110
100
90
80
70
60
50
40
30
20
10
0
-1000
0
1000
2000
3000
4000
5000
6000
7000
8000
9000
10000
11000
12000
13000
14000
15000

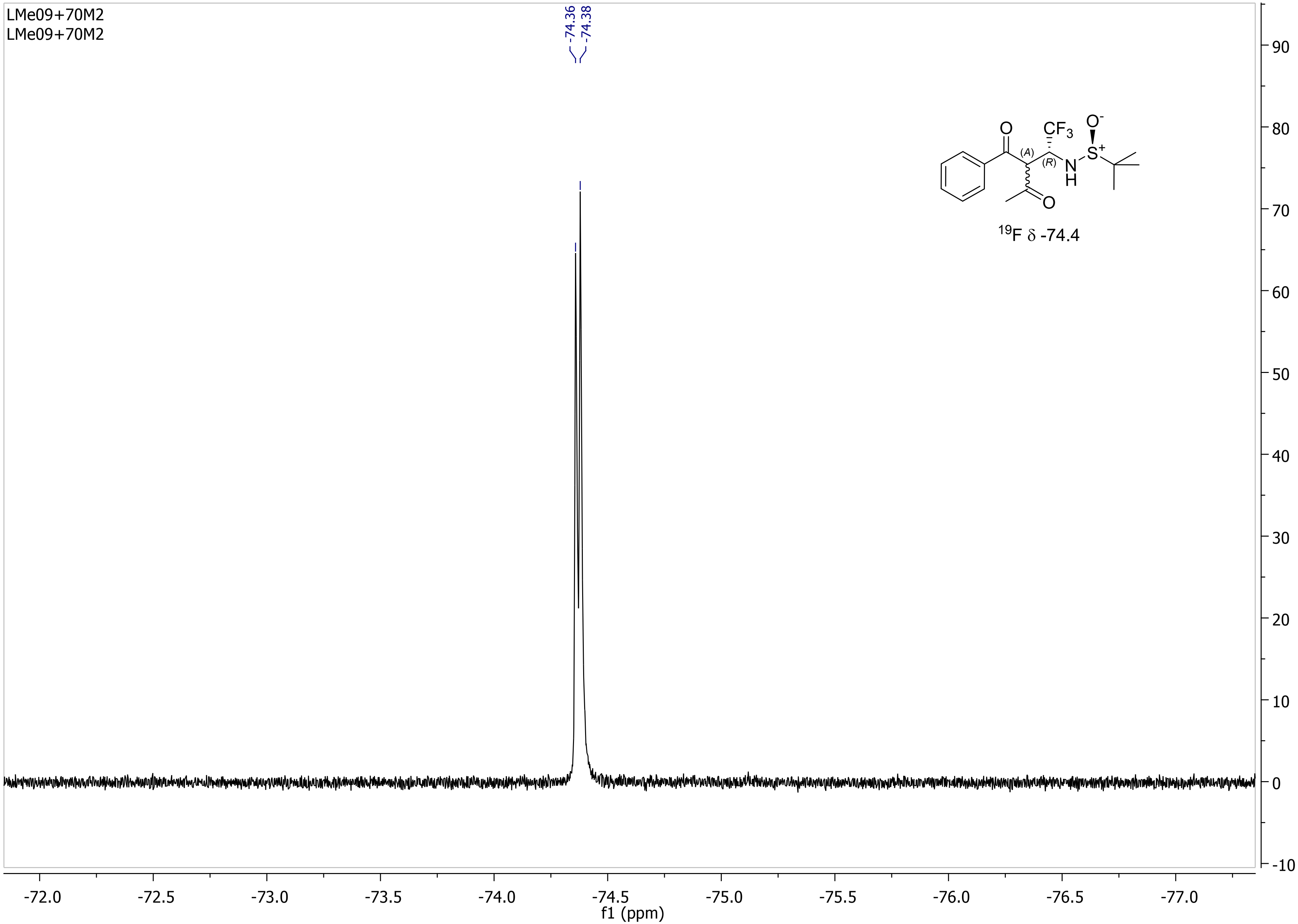
LMe09+70M2
LMe09+70M2
-74.36
-74.38
O
CF3
O-
(A)
(R)
N
S+
H
O
19F δ -74.4
-72.0
-72.5
-73.0
-73.5
-74.0
-74.5
-75.0
-75.5
-76.0
-76.5
-77.0
f1 (ppm)
90
80
70
60
50
40
30
20
10
0
-10

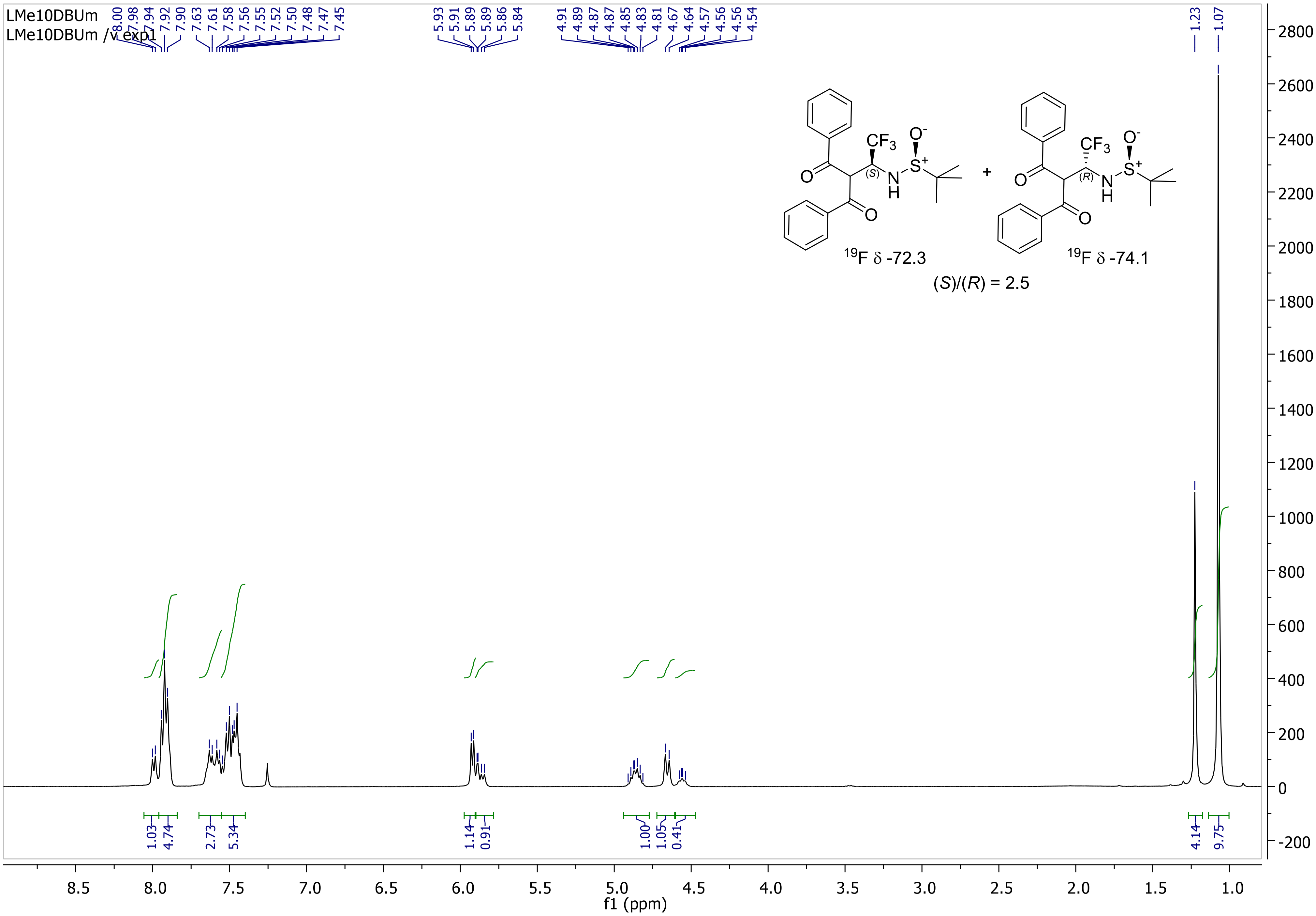
LMe10DBUm
LMe10DBUm /v exp1
8.00
7.98
7.94
7.92
7.90
7.63
7.61
7.58
7.56
7.55
7.52
7.50
7.48
7.47
7.45
5.93
5.91
5.89
5.89
5.86
5.84
4.91
4.89
4.87
4.87
4.85
4.83
4.81
4.67
4.64
4.57
4.56
4.56
4.54
1.23
1.07
CF3
O-
S+
(S)
N
H
O
O
+
CF3
O-
S+
(R)
N
H
O
O
19F δ -72.3
19F δ -74.1
(S)/(R) = 2.5
1.03
4.74
2.73
5.34
1.14
0.91
1.00
1.05
0.41
4.14
9.75
8.5
8.0
7.5
7.0
6.5
6.0
5.5
5.0
4.5
4.0
3.5
3.0
2.5
2.0
1.5
1.0
f1 (ppm)
2800
2600
2400
2200
2000
1800
1600
1400
1200
1000
800
600
400
200
0
-200

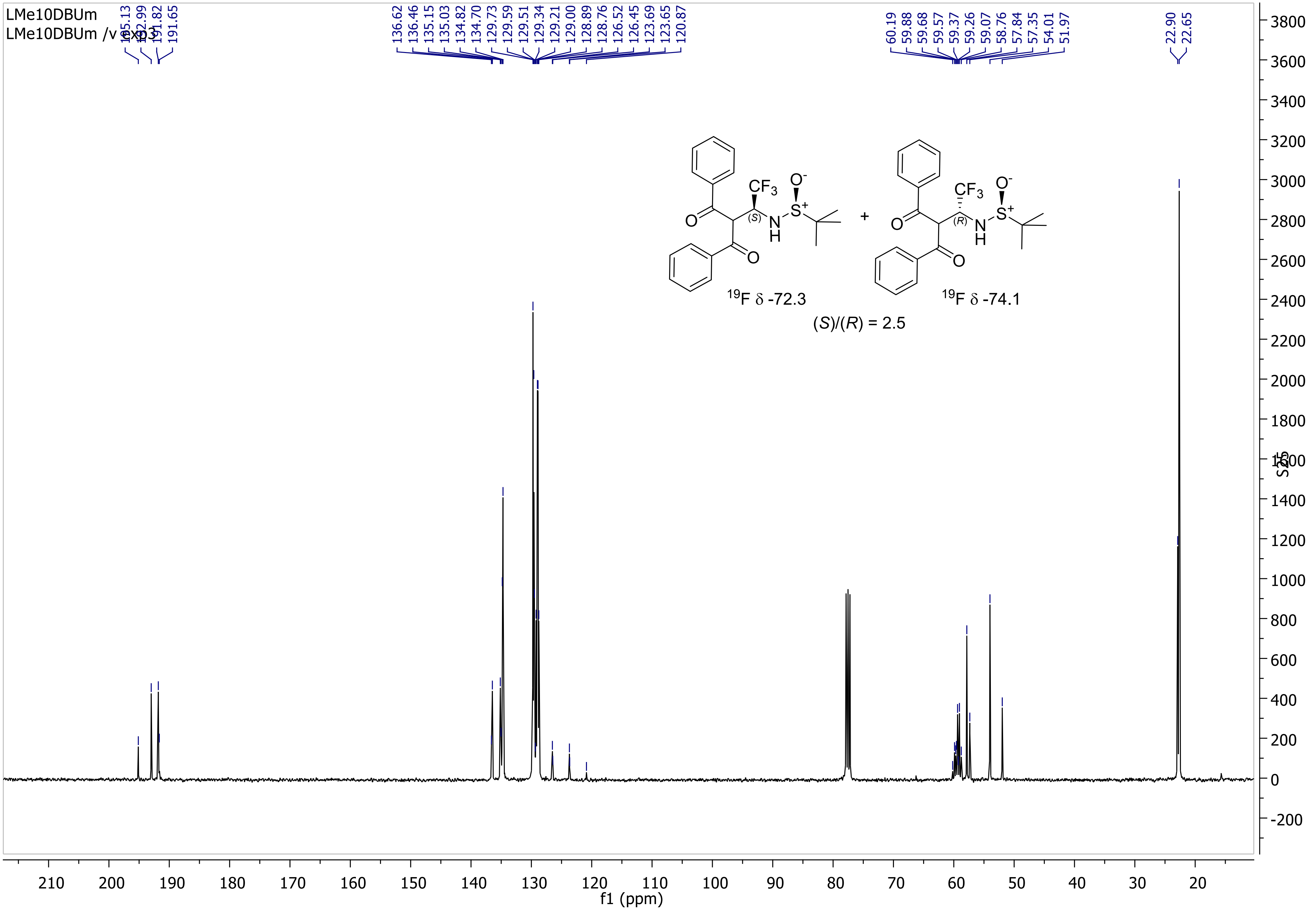
LMe10DBUm
LMe10DBUm /v exp3
195.13
192.99
191.82
191.65
136.62
136.46
135.15
135.03
134.82
134.70
129.73
129.59
129.51
129.34
129.21
129.00
128.89
128.76
126.52
126.45
123.69
123.65
120.87
60.19
59.88
59.68
59.57
59.37
59.26
59.07
58.76
57.84
57.35
54.01
51.97
22.90
22.65
CF3
O-
S+
N
H
O
(S)
(R)
+
19F δ -72.3
19F δ -74.1
(S)/(R) = 2.5
3800
3600
3400
3200
3000
2800
2600
2400
2200
2000
1800
1600
1400
1200
1000
800
600
400
200
0
-200
210
200
190
180
170
160
150
140
130
120
110
100
90
80
70
60
50
40
30
20
f1 (ppm)

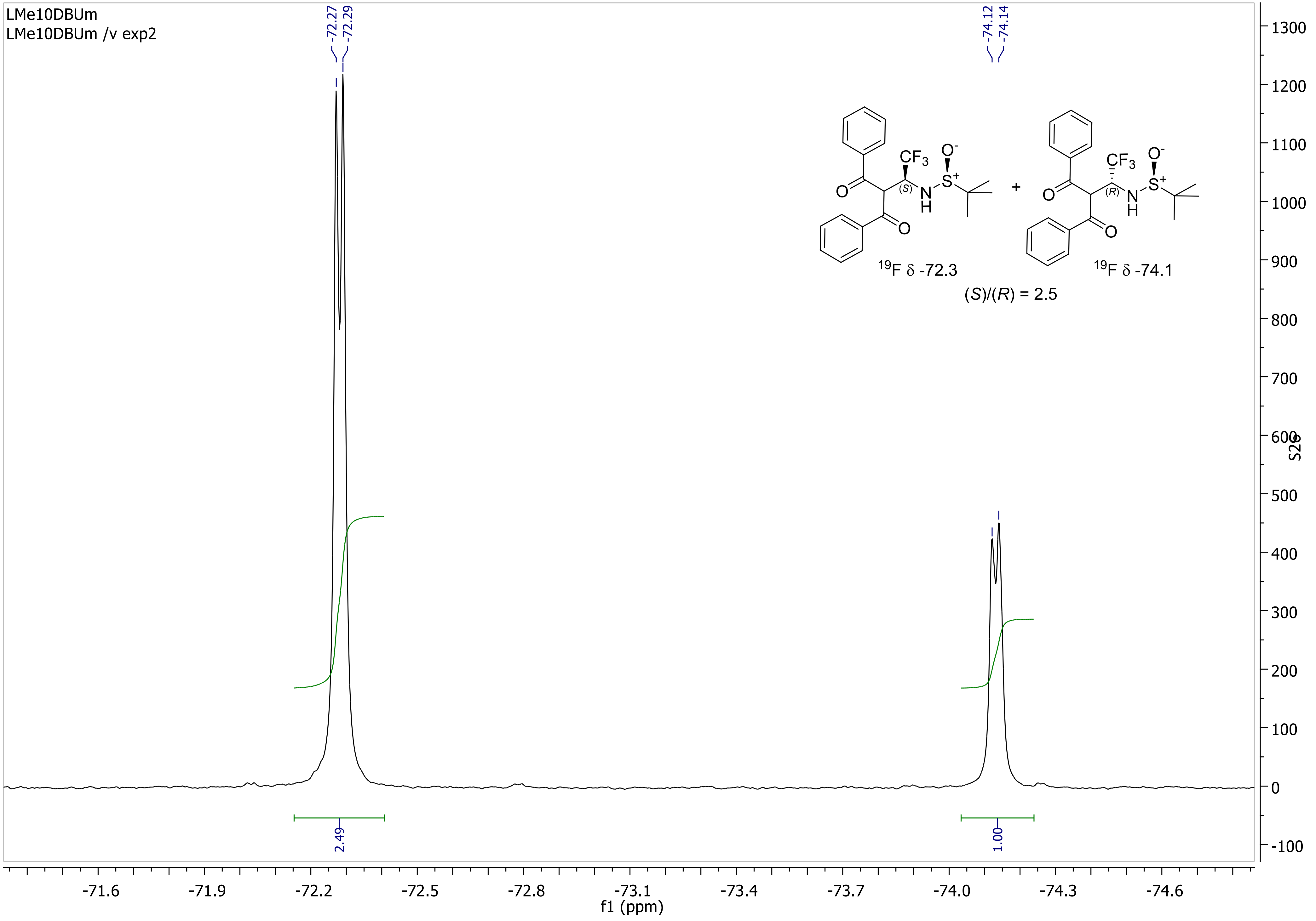
LMe10DBUm
LMe10DBUm /v exp2
-72.27
-72.29
-74.12
-74.14
CF3
O-
S+
(S)
N
H
O
O
+
(R)
^{19}F δ -72.3
^{19}F δ -74.1
(S)/(R) = 2.5
2.49
1.00
1300
1200
1100
1000
900
800
700
600
500
400
300
200
100
0
-100
-71.6
-71.9
-72.2
-72.5
-72.8
-73.1
-73.4
-73.7
-74.0
-74.3
-74.6
f1 (ppm)

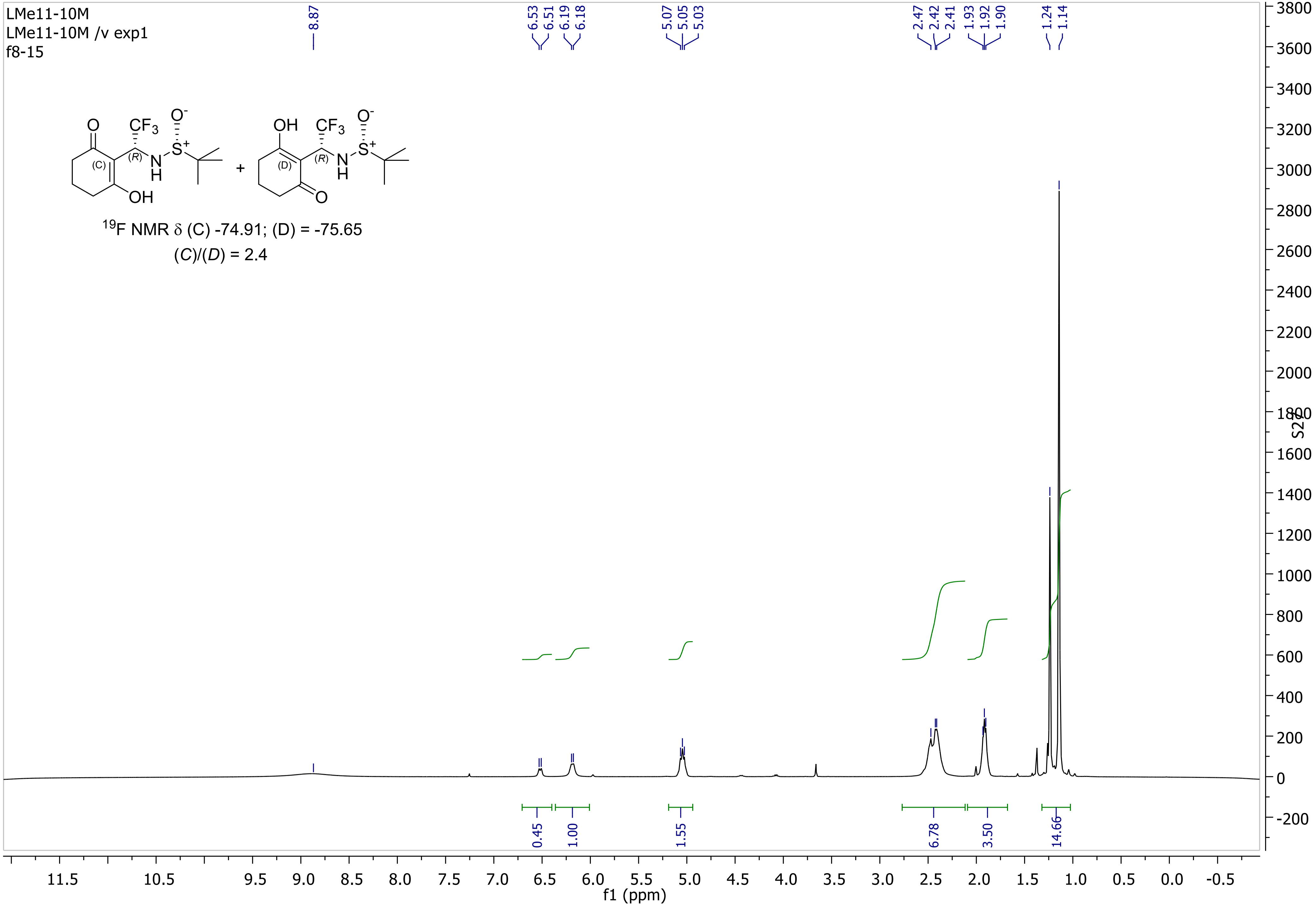

^{19}F NMR δ (C) -74.91; (D) = -75.65

(*C*)/(*D*) = 2.4

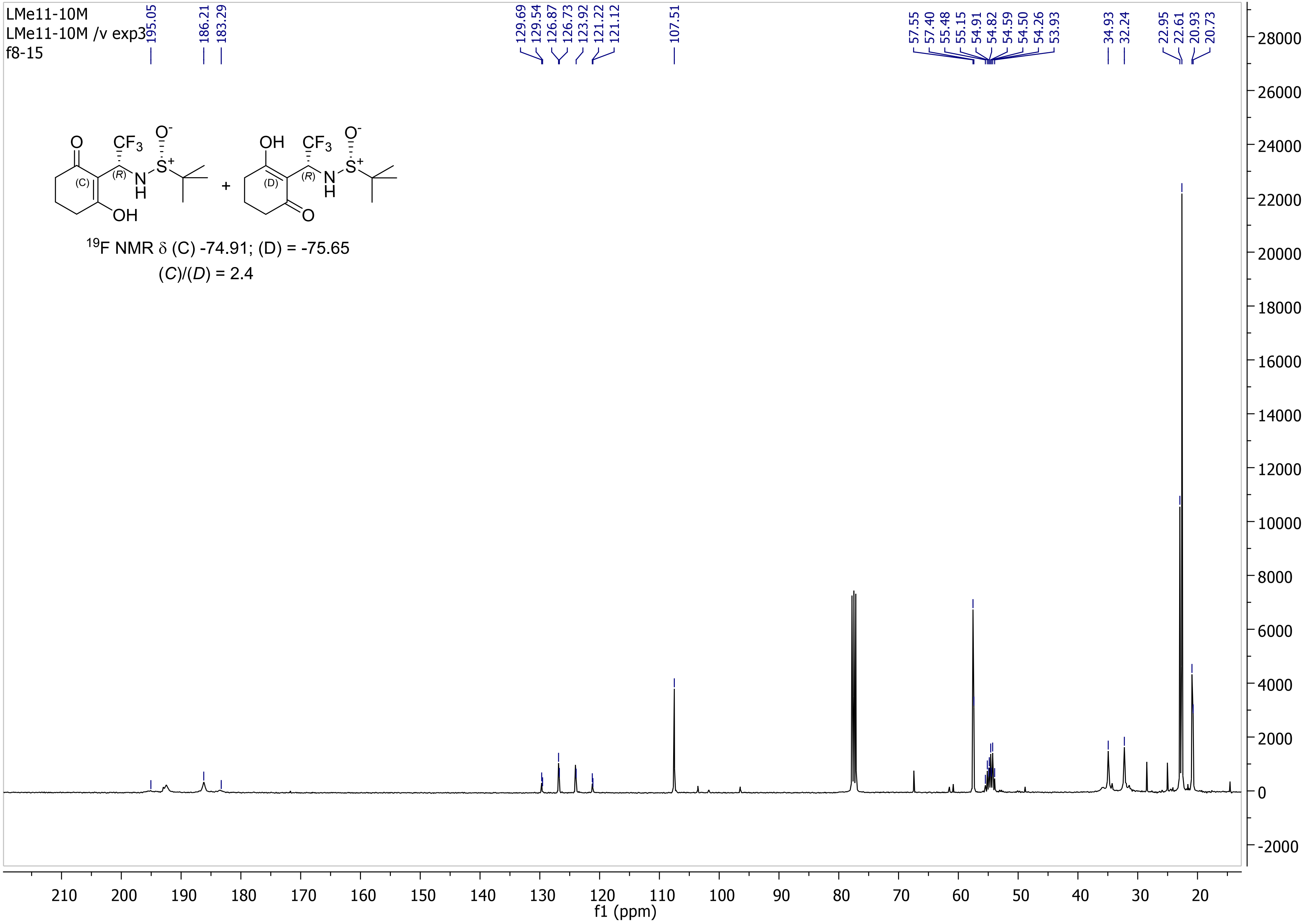

^{19}F NMR δ (C) -74.91; (D) = -75.65

(*C*)/(*D*) = 2.4

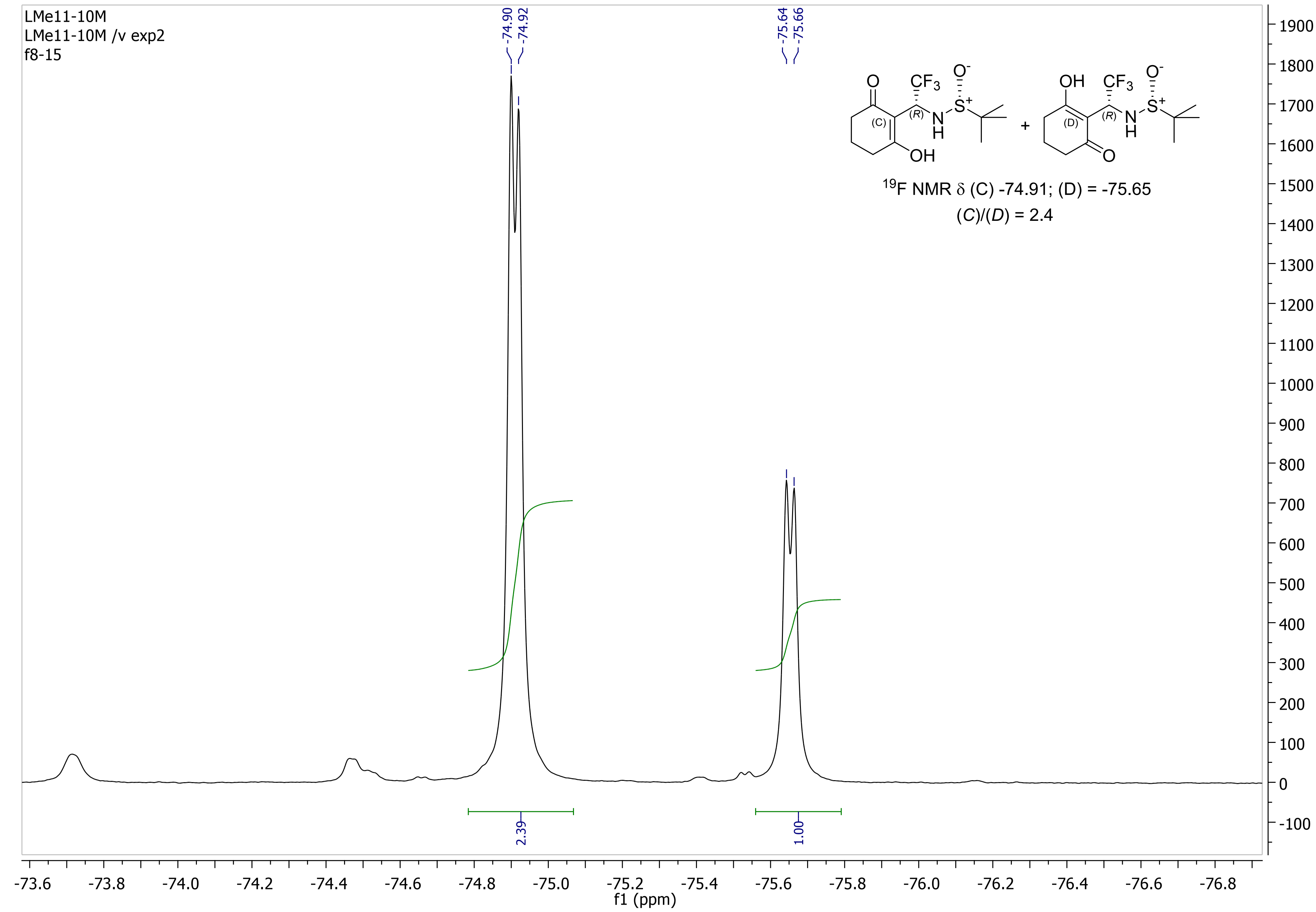

^{19}F NMR δ (C) -74.91; (D) = -75.65

(*C*)/(*D*) = 2.4

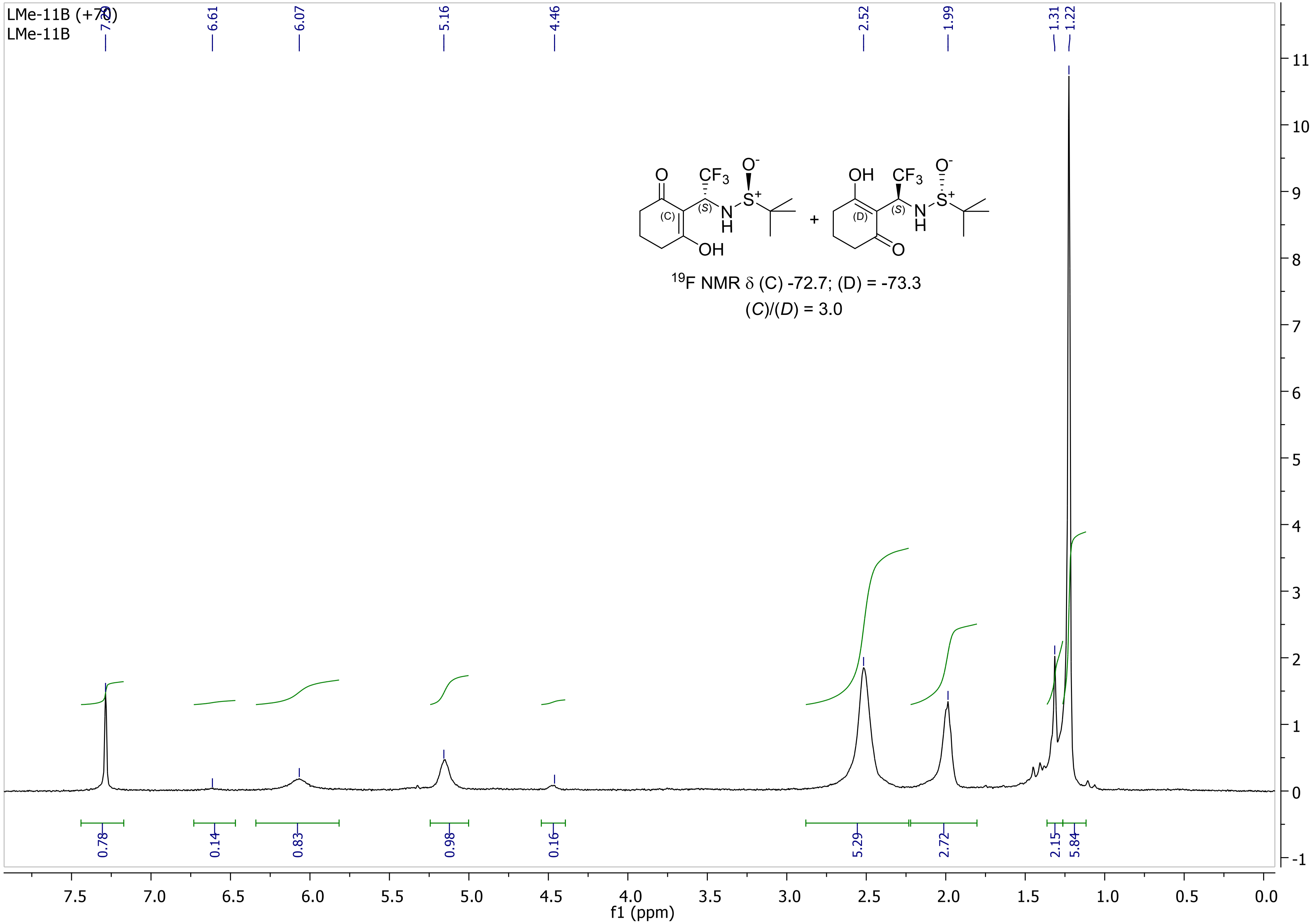

^{19}F NMR δ (C) -72.7; (D) = -73.3

(*C*)/(*D*) = 3.0

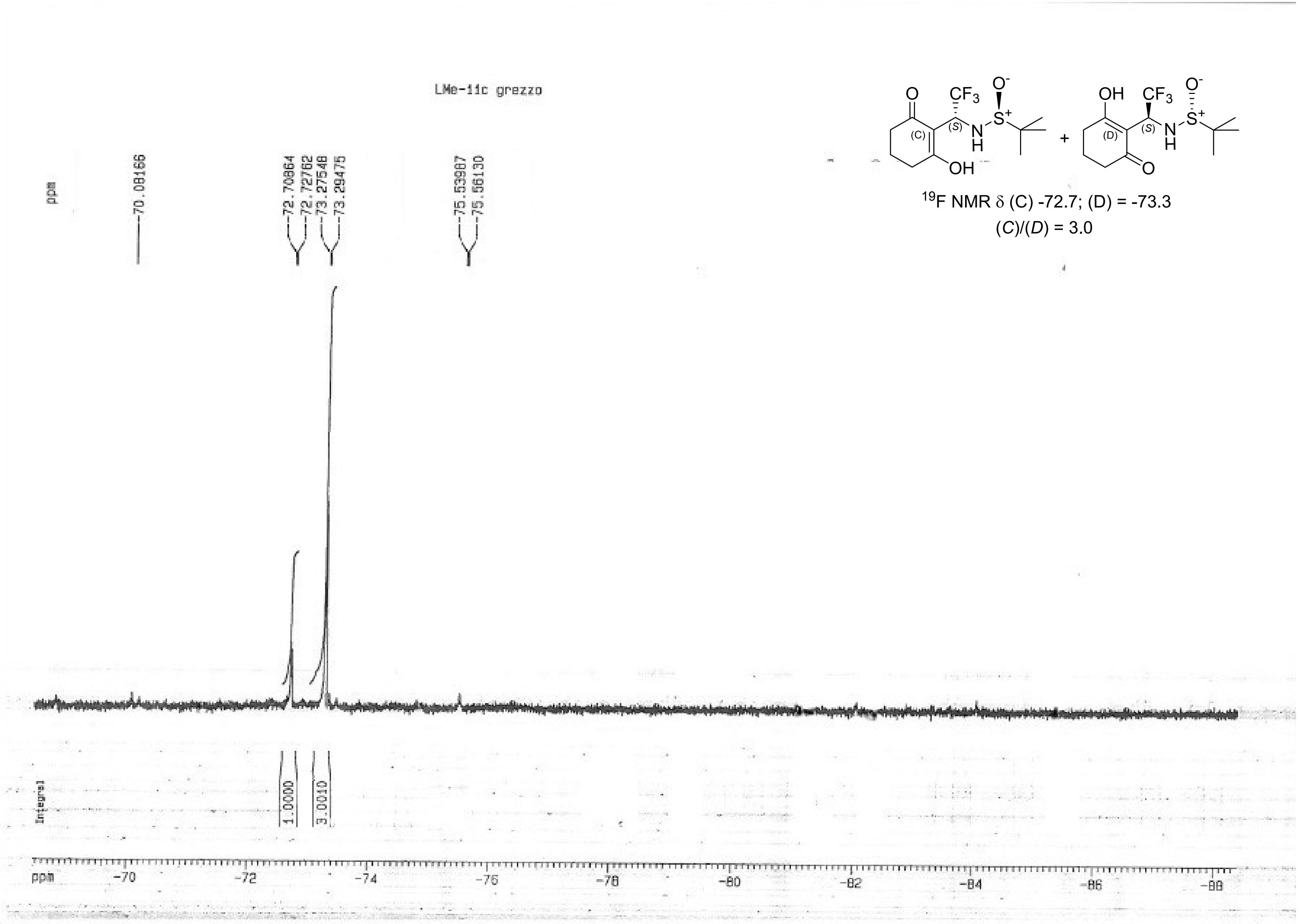

^{19}F NMR δ (C) -72.7; (D) = -73.3
(*C*)/(*D*) = 3.0

Chiroptical Spectroscopies

1) VCD Spectra

VCD spectra of $CDCl_3$ solutions (*ca* 0.1 M) were recorded on a Jasco FVS600 FTIR spectropolarimeter, in the range 950–1800 cm^{-1}, using 200 μm BaF_2 IR cells. 5000 scans were effected for each measurement. VCD spectra of the solvent was recorded in the same experimental conditions and then subtracted. All data are reported in Δε *vs* ν (cm^{-1}).

2) ORD Spectra

The ORD measurements of $CHCl_3$ solutions (~ 0.35 g/100mL) were carried out at 25 °C with a Jasco P-2000 Polarimeter. A 10 cm SiO_2 cuvette was employed in all cases. Five wavelengths were considered for Optical Rotations (OR), 589 nm (Na lamp), 546, 435, 405, and 365 nm (Hg lamp). OR data were obtained with ten measurements per wavelength after subtraction of the OR data of the solvent at the each wavelength. Specific rotation values were obtained from a program of the instrument software. The experimental data at two adjacent wavelengths were connected through a straight line.

3) ECD Spectra

ECD spectra of CH_3CN solutions (*ca.* 3.5×10^{-3} M) were recorded on a Jasco 815SE spectropolarimeter, in the range 400–185 nm, using 0.1 mm quartz cylindrical cuvettes. The average of 10 scans for each measurement was considered. ECD spectra of the solvent, taken in the same experimental conditions were then subtracted. Data are reported in Δε vs. λ (nm).

4) Computational Methods

Conformational analysis of **3a** as (S_C,S_S) and (R_C,S_S) was carried out at the MM level, with allowance of all conformer in the range 0-10 kcal/mol from the most stable one. All these conformers were fed into Gaussian09 [1] and DFT calculated conformers and IR and VCD spectra were obtained at M062x/TZVP and B3LYP/TZVP level within the PCM approximation.[2] All chiroptical properties were calculated as Boltzmann average weighed over conformer populations factors obtained according to both free energy (ΔG) and electronic energy (ΔE). All calculations showed no appreciable differences between free and electronic energy average representations; then all calculated spectra are reported as ΔG average. Only VCD B3LYP functional calculations exhibited differences between free ΔG and ΔE in some representations (see comment section). VCD-IR spectra simulation was obtained by assigning a Lorentzian band to each calculated transition, with assigned bandwidth of 10 cm^{-1}, for the rotational and dipole strengths calculated through Gaussian09. Scaling factor of 0.97 was applied to the calculated VCD bands. ECD calculated spectra were obtained by Gaussian09 using respectively CAM-B3LYP/TZVP and M06x/TZVP levels of theory. ECD Spectra were simulated assigning Gaussian bands to each electronic calculated transition with 0.2 eV wide Gaussian bands. All calculated ECD and UV absorption transitions were shifted by 10 nm. The first 50 excited states were considered in setting up the calculation.

Comments on the VCD-IR, ORD and ECD analysis and computational methods for the assignment of the absolute configuration

The AC on the $-C^*HCF_3$ stereogenic carbon generated in the synthesis of **3a** has been investigated by comparison of experimental chiroptical spectroscopies, namely VCD, ECD and ORD, with DFT respective computed properties. [3-5] This approach resulted to be quite robust for stereochemical characterization and it was recently applied on some $-CF_3$ substituted organic compounds. [6-8]

Vibrational Circular Dichroism Analysis

Experimental VCD spectra of the four stereoisomers of **3a** show a strong and clear correlation between the C=O stretching related bands and the *X*/*Y* absolute configuration (AC) of the stereogenic carbon (Fig. 1). The spectra exhibit a bisignated couplet-like band centered at ca. 1720 cm^{-1} with a positive-negative doublet (considered from lower to higher wavenumbers) related to the *X* AC and *vice versa* for *Y* AC.

It can be noted that even in the MID-IR region VCD spectra appear to be affected by the carbon chirality only. The comparison of VCD spectra of the two couples of diastereomers (*Y,Rs*)-**3a**/(*X,Rs*)-**3a** and (*Y,Ss*)-**3a**/(*X,Ss*)-**3a** exhibiting the same AC at sulfur atom is shown in Fig. SI-1 (right panels).

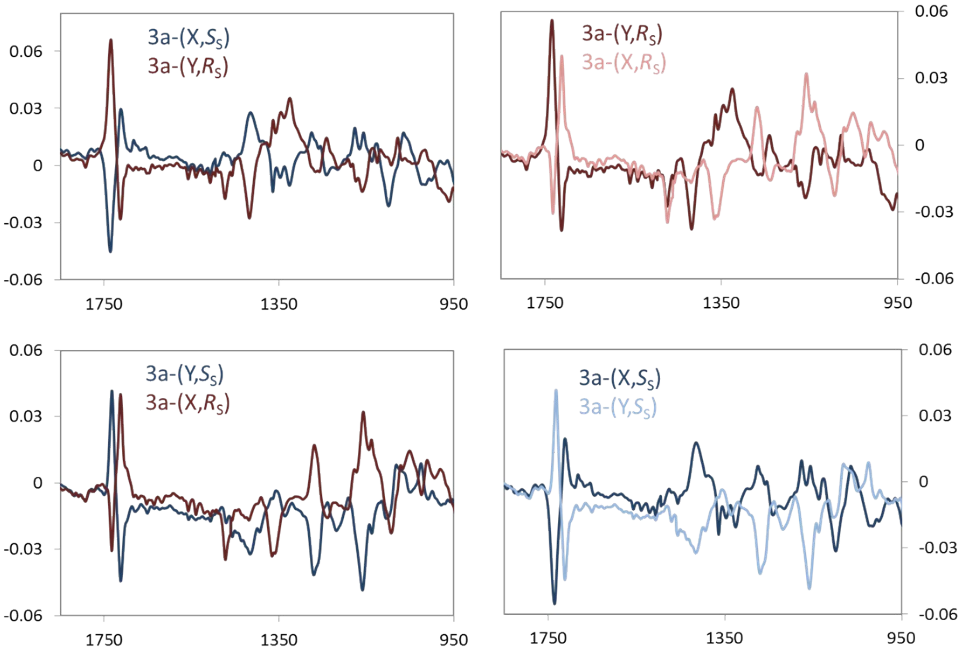

Figure SI-1. Experimental VCD of both couple of enantiomer of **3a** (left panel). Comparisons of experimental VCD spectra of **3a** isomers grouped by sulfur atom AC (right panel).

The VCD spectra in the 950-1500 cm^{-1} range are substantially mirror image of each other, proving the major influence of the chiral carbon over the whole vibrational optical activity effects (for details of VCD and IR spectra see Fig SI-2)

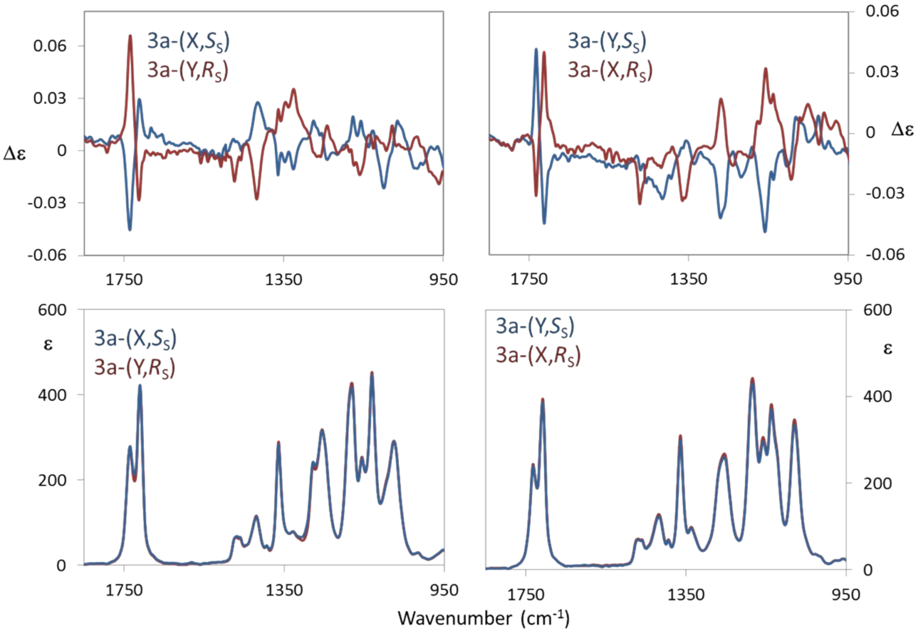

Figure SI-2. Experimental IR and VCD of (*Y*,*R*$_S$)-**3a** vs (*X*,*S*$_S$)-**3a**, left, and (*X*,*R*$_S$)-**3a** *vs* (*Y*,*S*$_S$)**-3a**, right, in deuterated chloroform solution (0.079 M, 0.081M, 0.084M and 0.082M respectively) in 200 mm cell. 5000 accumulation scans.

Calculations were performed by setting as (*S*) the AC at the sulfur atom and considering both (*S*,*S*$_S$) and (*R*,*S*$_S$) as the possible configurations to be compared with the experimental data. Molecular Mechanics (MM) by means of MMFF94s force field, predict the existence of 63 conformers of (*S*,*S*$_S$)-**3a** and 55 conformers of (*R*,*S*$_S$)-**3a** within 10 kcal/mol energy window (Table 1).

Table SI-1. Relative energies and population distributions of the conformers of each diastereomer (*S*,*S*$_S$)-**3a** and (*R*,*S*$_S$)-**3a** calculated at DFT/M062X/TZVP/PCM (chloroform) level approximation.

Conformer	ΔG (kcal/mol)	% pop	ΔE (kcal/mol)	% pop
(*S*,*S*$_s$)-1	0.00	49.7	0.00	42.8
(*S*,*S*$_s$)-2	0.51	21.0	0.38	22.5
(*S*,*S*$_s$)-3	0.94	10.2	0.58	16.1
(*S*,*S*$_s$)-4	1.07	8.2	1.59	2.9
(*S*,*S*$_s$)-5	1.13	7.4	1.61	2.8
(*S*,*S*$_s$)-6	2.05	1.6	0.94	8.7
(*S*,*S*$_s$)-7	2.08	1.5	2.23	1.0
(*S*,*S*$_s$)-8	3.06	0.3	2.09	1.2
(*S*,*S*$_s$)-9	3.44	0.1	1.84	1.9

Conformer	ΔG (kcal/mol)	% pop	ΔE (kcal/mol)	% pop
(*R*,*S*$_s$)-1	0.00	52.0	0.00	52.8
(*R*,*S*$_s$)-2	0.91	11.2	1.22	6.8
(*R*,*S*$_s$)-3	0.98	10.0	1.35	5.4
(*R*,*S*$_s$)-4	1.10	8.1	1.08	8.6
(*R*,*S*$_s$)-5	1.28	6.0	1.39	5.1
(*R*,*S*$_s$)-6	1.54	3.8	1.19	7.0
(*R*,*S*$_s$)-7	1.56	3.7	1.16	7.5
(*R*,*S*$_s$)-8	1.97	1.9	1.89	2.2
(*R*,*S*$_s$)-9	2.19	1.3	2.25	1.2
(*R*,*S*$_s$)-10	2.26	1.1	2.31	1.1
(*R*,*S*$_s$)-11	2.57	0.7	2.35	1.0
(*R*,*S*$_s$)-12	3.21	0.2	2.19	1.3

All the possible conformations were then further optimized by means of DFT at M062x/TZVP/PCM (chloroform) level of theory for VCD analysis. Frequency calculations were also performed at the same level of theory; no imaginary frequencies were found, so, all conformations are real minima.

Fig. SI-3 shows the comparison of experimental VCD spectra of (X,S_S)-**3a** (left panel) and (Y,S_S)-**3a** (right panel) with the calculated (S_C,S_S) and (R_C,S_S) in the range 1850–1650 cm^{-1}. It can be noted that the positive-negative doublet at *ca.* 1720 cm^{-1} in the VCD spectrum of (X,S_S)-**3a**, relative to the C=O stretching, is well predicted in sign by the calculation for the (S_C,S_S) configuration.

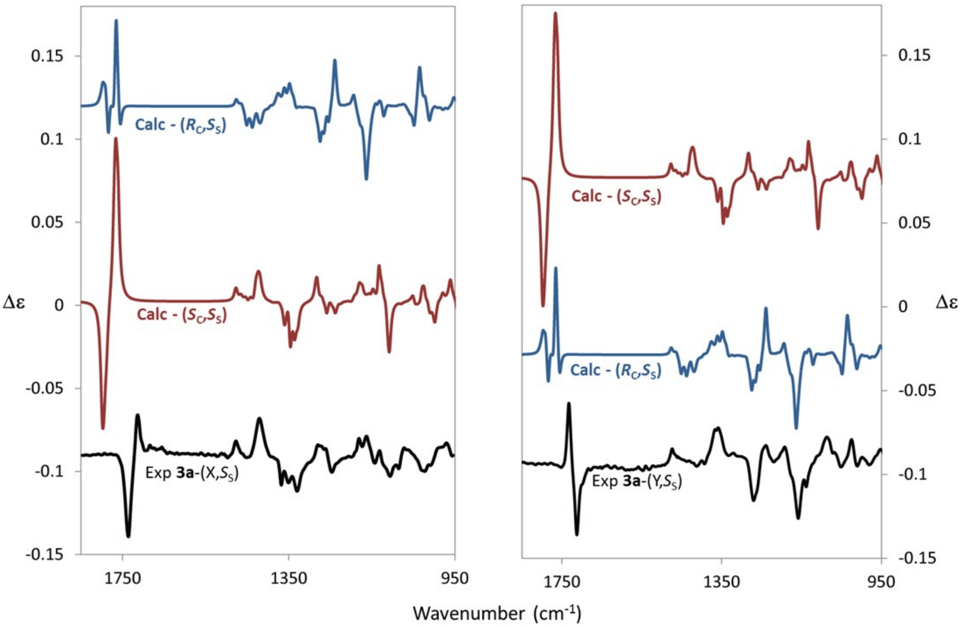

Figure SI-3. Experimental VCD of (X,S_S)-**3a** (left panel) and (Y,S_S)-**3a** (right panel), reported as semi-difference, compared with both calculated (S_C,S_S) and (R_C,S_S) diastereomers (as Boltzmann weighed average) at M062X/TZVP/PCM($CHCl_3$) level.

The positive component of the doublet at low energy is ascribed to the antisymmetric stretching mode of the two carbonyl groups, while the negative one, at higher frequency, is ascribed to the corresponding symmetric mode. The calculated VCD spectra of the conformers of both diastereomer (*S*,*S*$_S$)-**3a** and (*R*,*S*$_S$)-**3a** are compared with the experimental VCD spectra of (*X*,*S*$_S$)-**3a** and (*Y*,*S*$_S$)-**3a** in the C=O stretching region (1650–1850 cm^{-1}) (Figs SI-4 and SI-5, respectively).

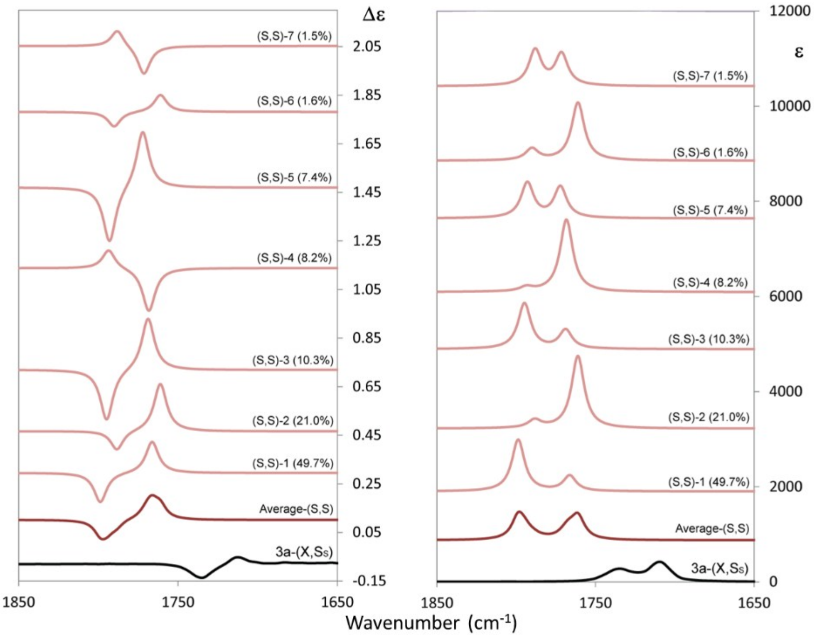

Figure SI-4. Calculated VCD (left) and IR (right) spectra of the first seven conformers of (*S*,*S*$_S$)-**3a** (99.6% of overall population), in the range of 1650–1850 cm^{-1}, compared with experimental (black) and Boltzmann's average calculated (brown) spectra. Relative population percentages are reported in brackets. Calculations were performed at DFT/M062x/TZVP. Scaling factor 0.97.

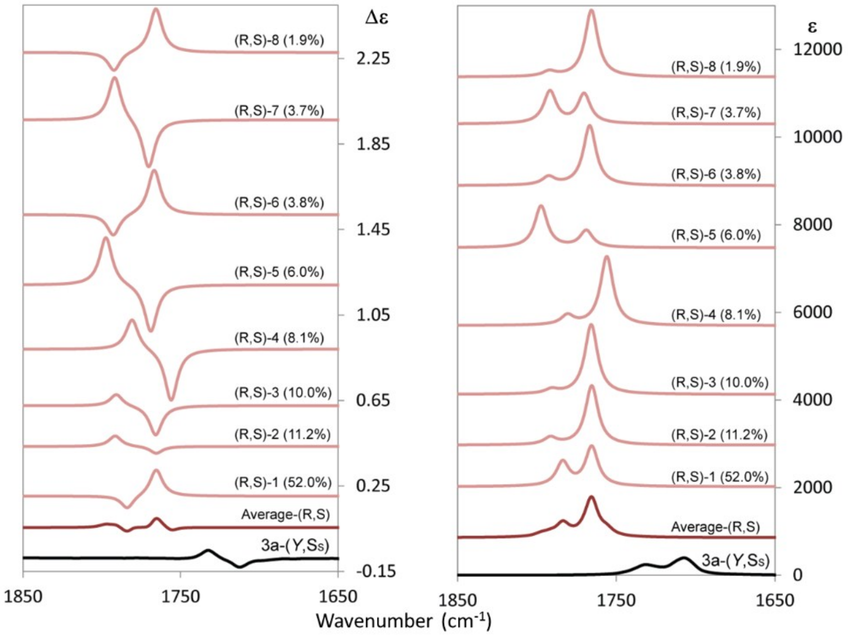

Figure SI-5. Calculated VCD (left) and IR (right) spectra of the first eight (*R*$_C$,*S*$_S$) conformers (96.7% of overall population), in the range of 1650-1850 cm^{-1}, compared with experimental and Boltzmann's averaged calculated spectra. Relative population percentages are reported in brackets. Calculations were performed at DFT/M062x/TZVP. Scaling factor 0.97.

Noteworthy, five of the seven most populated conformations (about 90% of overall population) possess a positive-negative doublet.

This picture strongly supports the (*S*) configuration of the stereogenic carbon previously marked with the unknown (*X*), confirming the carbonyl stretching mode as a good vibrational probe for carbon chirality of **3a**. Conversely, the negative-positive doublet at 1720 cm^{-1} of (Y,S_S)-**3a** should be properly predicted as (R,S_S)-**3a** by (R_C,S_S) calculation. Unfortunately the calculated VCD spectrum of the (R_C,S_S) diastereomer in the C=O stretching region experiences a strong conformational effect leading to a multiple-component band arising from the Boltzmann averaged spectrum which is difficult to relate to the experimental one.

Fig. SI-5 shows the comparison VCD spectra of each (R_C,S_S) conformers with the experimental (Y,S_S)-**3a** in the C=O stretching region (1650-1850 cm^{-1}). We can see that the spectrum of most of the conformers (30% of the overall population) have the same negative-positive trend as the experimental one. On the contrary, the spectrum of the most populated conformer (51% of the population) exhibits opposite trend with respect to the experimental data. B3LYP functional was also employed to calculate geometries, frequencies, Boltzmann distribution and VCD-IR spectra of **3a** in the same basis set conditions (for details see Table SI-2).

Table SI-2. Conformers calculated relative energies and populations percentage distributions for compound **3a** according to (S_C,S_S) and (R_C,S_S) possible diastereomers at DFT/B3LYP/TZVP level in chloroform PCM approximation.

Conformer	ΔG	% pop	ΔE	% pop
(*S*,*S*)-1	0.00	28.8	0.91	6.1
(*S*,*S*)-2	0.19	20.9	0.22	19.5
(*S*,*S*)-3	0.53	11.8	0.48	12.7
(*S*,*S*)-4	0.53	11.7	0.49	12.4
(*S*,*S*)-5	0.73	8.4	0.00	28.3
(*S*,*S*)-6	0.91	6.2	1.03	4.9
(*S*,*S*)-7	0.98	5.5	0.74	8.1
(*S*,*S*)-8	1.01	5.3	0.98	5.4
(*S*,*S*)-9	2.04	0.9	1.68	1.7
(*S*,*S*)-10	2.40	0.5	1.95	1.0

Conformer	ΔG	% pop	ΔE	% pop
(*R*,*S*)-1	0.00	38.7	0.80	11.4
(*R*,*S*)-2	0.04	36.4	0.00	43.8
(*R*,*S*)-3	0.45	18.2	0.03	41.8
(*R*,*S*)-4	1.33	4.1	2.01	1.5
(*R*,*S*)-5	1.90	1.6	2.46	0.7
(*R*,*S*)-6	2.10	1.1	2.37	0.8

Conformational effect is still experienced in the C=O stretching region even though the calculated spectrum is less structured with respect to the one obtained with M062x functional and the ΔE average exhibits a quite better VCD profile than the ΔG one (Fig. SI-6).

However, the MID-IR 950-1550 cm^{-1} region reveals a bad matching of the experimental VCD spectrum of the (Y,S_S)-**3a** with the calculated VCD spectrum, confirming M06-2X functional as the best choice in our approach. The comparison of calculated VCD and IR spectra of each (S_C,S_S) and (R_C,S_S) conformer with the experimental spectra of (X,S_S)-**3a** and (Y,S_S)-**3a** in the MID-IR region (950-1550 cm^{-1}) are shown in Figs. SI-7 and SI-8. Noteworthy, the calculated VCD spectrum of (S_C,S_S) fits the experimental (X,S_S)-**3a** spectrum qualitatively better than the calculated (R_C,S_S) do (Figure SI-7 left panel), while the latter fits much better the experimental spectrum of (Y,S_S)-**3a**.

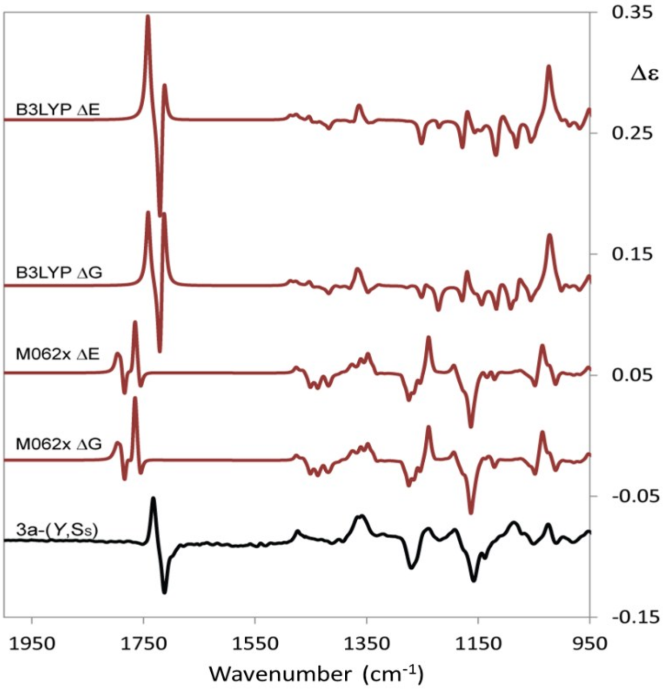

Figure SI-6. Experimental VCD of (*Y*,S_S)-**3a**, reported as semi-difference, compared with calculated (R_C,S_S) diastereomer, as Boltzmann weighed average over free thermal energy ΔG and electronic energy ΔE, at M062x/TZVP/PCM($CHCl_3$)and B3LYP/TZVP/PCM($CHCl_3$) level. Scaling factor 0.97.

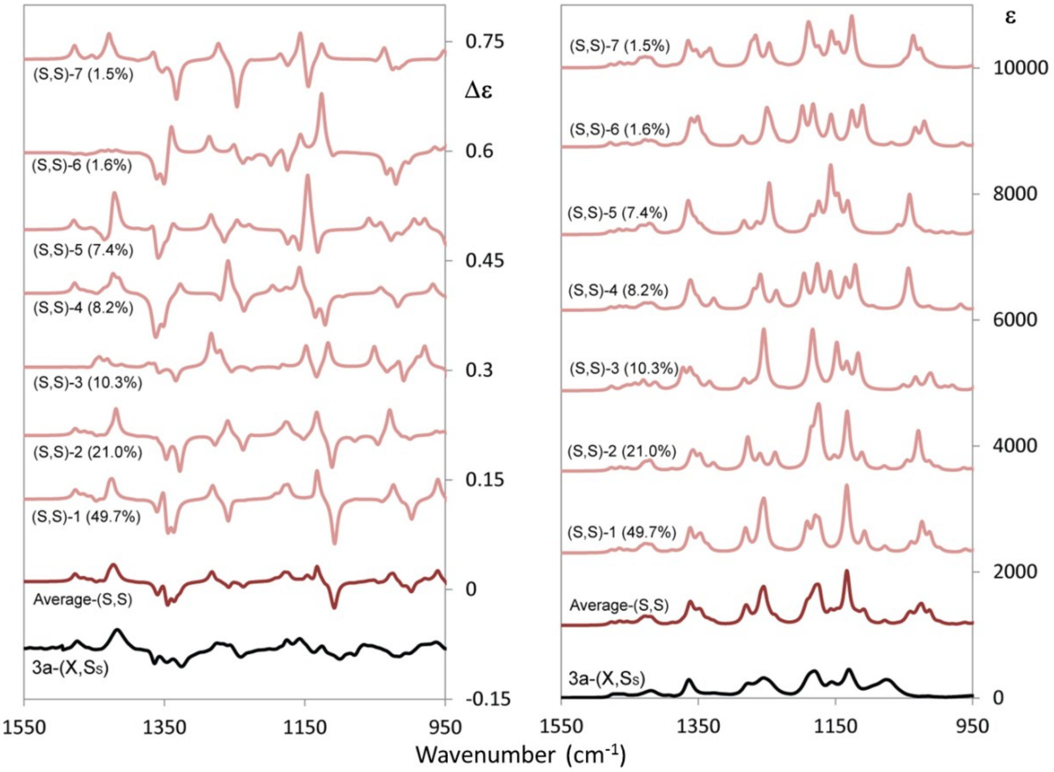

Figure SI-7. Calculated VCD (left) and IR (right) spectra of first seven (S_C,S_S) conformers (99.6% of overall population), in the range of 950-1550 cm^{-1}, compared with experimental and Boltzmann's averaged calculated spectra. Relative population percentages are reported in brackets. Calculations were performed at DFT/M062x/TZVP. Scaling factor 0.97.

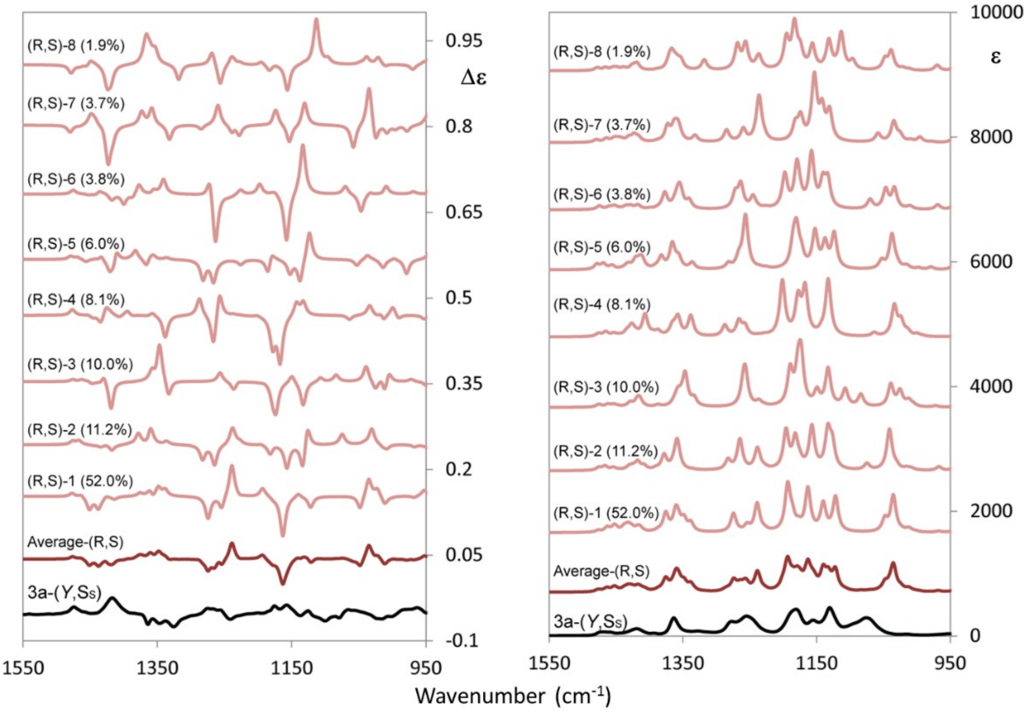

Figure SI-8. Calculated VCD (left) and IR (right) spectra of first eight (R_C,S_S) conformers (96.7% of overall population), in the range of 950-1550 cm^{-1}, compared with experimental and Boltzmann's averaged calculated spectra. Relative population percentages are reported in brackets. Calculations were performed at DFT/M062X/TZVP. Scaling factor 0.97.

To confirm the performance of calculated VCD spectra in discriminating the two **3a** diastereomers ACs, the similarity index (S.I.) [9] and Sim_NN [10] was computed over the 950-1550 cm^{-1} frequency range. [11-13] The S.I. index varies between −1 (wrong AC assignment) and +1 (correct AC assignment). It should be remarked that S.I. is not intensity sensitive, while Sim_NN it is. Results are summarized in Table SI-3.

The two indices were inferred using different empirical scaling factors (1, which means that no scaling factor is applied, 0.98 and 0.97). The scaling factor which maximizes all indices (in absolute values) was found to be 0.97. For (X,S_S)-**3a** S.I. and Sim_NN, correlated with the (S_C,S_S) calculation, are +0.65 and +0.47 respectively; –0.44 and –0.28 are the indices values correlated to (R_C,S_S). S.I. and Sim_NN parameters for (Y,S_S)-**3a** were –0.31 and –0.18 for (S_C,S_S) and +0.69 and +0.52 for (R_C,S_S) calculation, respectively. These results allow us to confirm unambiguously the previous assignment, namely: *X*→*S* and *Y*→*R*.

Table SI-3. Values of Similarity Indices *S.I.* and *Sim*_NN of Computed (for the two possible S_S stereoisomers) and Experimental VCD of Compound **3a**. The last two indices values labelled as '**alt-**' refer to the calculated (R_C,S_S) obtained diastereomer neglecting the most populated conformer (*R*,*S*)-1 in the Boltzmann's distribution (see manuscript). For The Definition of *S.I.* [13] and *Sim*_NN [14].

	S.I. (S_C,S_S)	*Sim_NN* (S_C,S_S)	*S.I.* (R_C,S_S)	*Sim_NN* (R_C,S_S)	*S.I.* **alt**-(R_C,S_S)	*Sim_NN* **alt**-(R_C,S_S)
(*X*,S_S)-**3a**	+0.65	+0.47	-0.44	-0.28	-	-
(*Y*,S_S)-**3a**	-0.31	-0.18	+0.69	+0.52	+0.60	+0.39

Fig. SI-9 shows the comparison between experimental VCD spectrum of (*Y*,S_S)**-3a** with the calculated VCD spectrum of (*R*,S_S)**-3a**, in which the most populated conformer exhibiting an opposite trend with respect to the experimental was neglected. The C=O doublet at 1720 cm^{-1} exhibits a negative-positive shape and the MID-IR region is not affected even if the computed S.I. and Sim_NN parameters decreased slightly to +0.60 and +0.39 respectively.

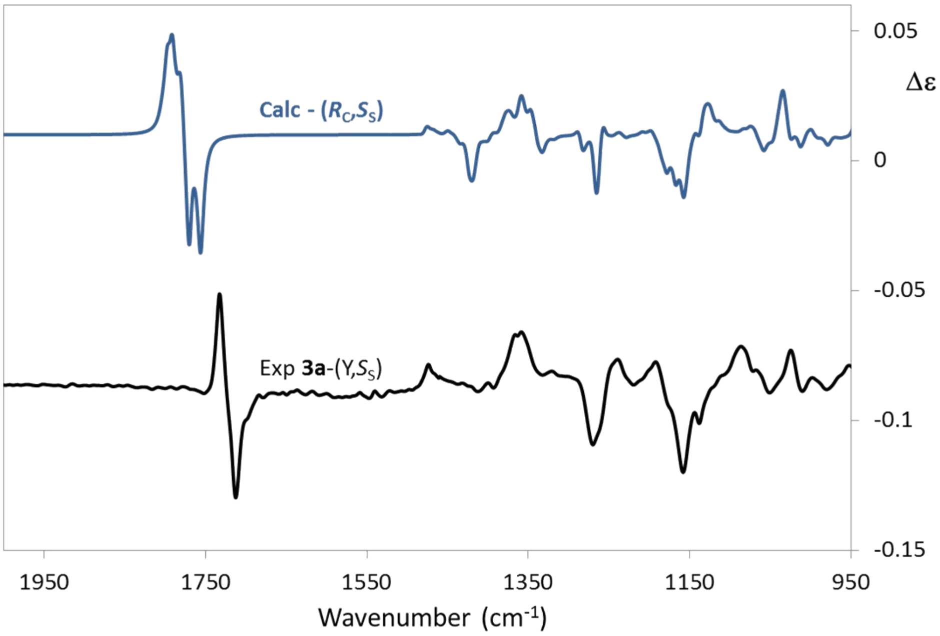

Figure SI-9. Experimental VCD of (*Y*,S_S)-**3a**, reported as semi-difference, compared with (R_C,S_S) diastereomer, as Boltzmann weighed average, neglecting conformer (*R*,*S*)-1 in the Boltzmann's distribution (see manuscript). M062x/TZVP/PCM($CHCl_3$) level. Scaling factor 0.97.

Electronic Circular Dichroism (ECD) and ORD analysis

Experimental ECD and ORD spectra as discrete wavelength specific optical rotation curve of the two couples of enantiomers of **3a** are shown in Fig. SI-10 (for detailed values see Table SI-4). All spectra profiles are in good enantiomeric relationship.

ECD spectra exhibit a Cotton effect (CE) centered at *ca.* 290 nm ascribed to n→π* C=O transition, a CE at ca. 220 nm related to alkyl sulfoxide n→π* transition [14-16] and a partially detectable CE which is outside the accessible experimental range. It is important to note that, as reported in Fig. SI-10 (middle panel), the CE at 290 nm are the ones sensitive to the inversion of the chirality on carbon atom due to the proximity of C=O group to the chiral center (positive CE for *X* and negative CE for *Y*), while the transition involved in 220 nm CE consistently preserves its sign with sulfur AC (positive CE for *R* and negative CE for *S*).

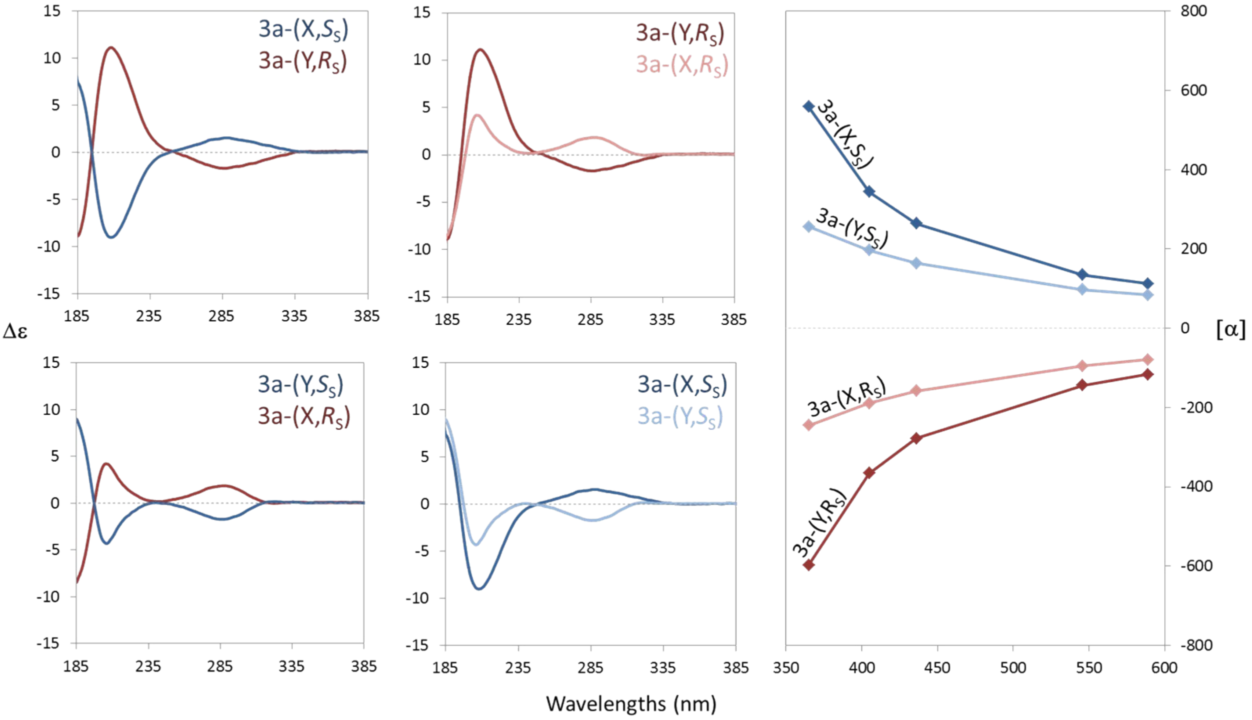

Figure SI-10. Experimental ECD of both couple of enantiomer of **3a** (left panel). Comparisons of experimental ECD spectra of **3a** isomers grouped by sulfur atom AC (middle panel). Comparison of ORD curves of the four **3a** stereoisomers (right panel).

Table SI-4. Experimental specific rotation of four stereoisomers of **3a** measured at five different wavelength (589, 546, 436, 405 and 365 nm) in chloroform solvent at concentration of ca. 0.35 g/100mL.

λ (nm)	(X,S_S)-**3a**	(Y,S_S)-**3a**	(X,R_S)-**3a**	(Y,R_S)-**3a**
589	+112	+84	-79	-116
546	+135	+97	-95	-144
436	+264	+164	-158	-278
405	+344	+197	-189	-366
365	+559	+256	-245	-597

Concerning the experimental ORD, it can be noted that, despite the well-known Kramers-Kronig relationship[17] between ECD and ORD, stating the sign of the ORD curve being determined by the lowest energy transition in the ECD spectrum, the curves for the two couples of diastereomers, which differ in the chirality of carbon atom, have the same sign. Both (X,S_S)-**3a** and (Y,S_S)-**3a** exhibit a positive ORD trend

(Fig. SI-10, right panel), although the lowest energy CEs in the corresponding ECDs are opposite in sign. Even the CEs at 220 nm (negative for both diastereomers) do not contribute to the overall positive trend of the two ORD curves. The same considerations hold for the diastereomers (X,R_S)-**3a** and (Y,R_S)-**3a**. It is also clear that the trend of ORD sign is totally driven by sulfur chirality and the relatively small difference between two diastereomers (i.e. *R,S* and *SS*), in order to discriminate X/Y AC, makes the detailed computational analysis of ORD too difficult in proportion to the information being drawn and is not worth presenting here.

The comparison of the experimental ECD spectra of (X,S_S)-**3a** (left panel) and (Y,S_S)-**3a** (right panel) with the calculated ones for (S_C,S_S) and (R_C,S_S) is shown in Fig. SI-11.

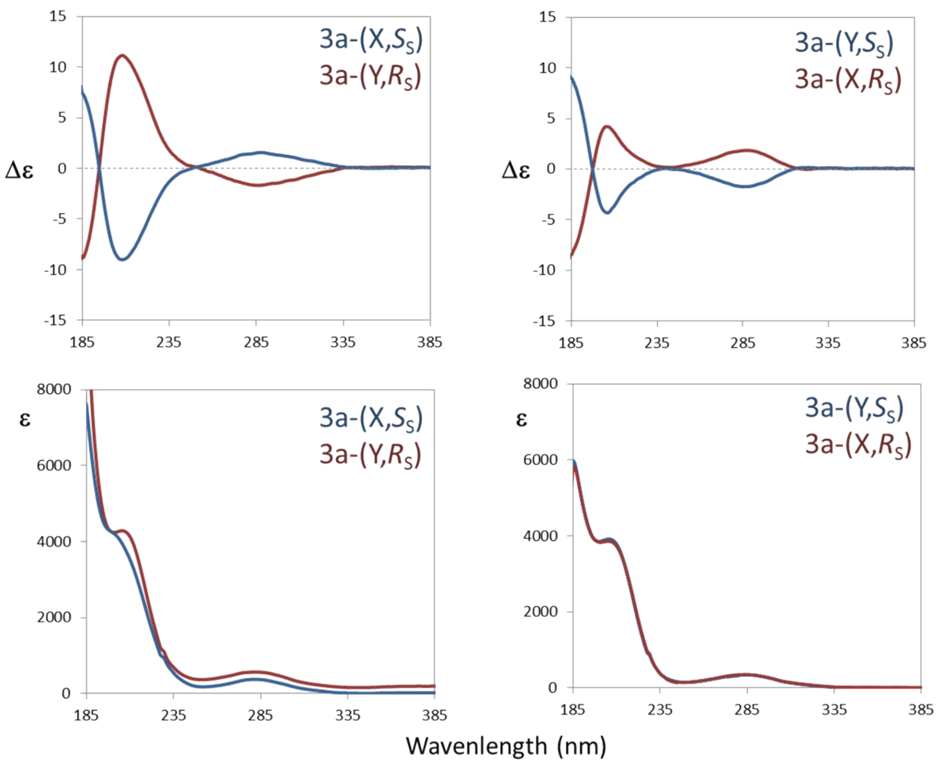

Figure SI-11. Experimental UV and ECD of **3a**-(Y,R_S) vs **3a**-(X,S_S), left, and **3a**-(X,R_S) vs **3a**-(Y,S_S), right, in acetonitrile solution (0.0032M, 0.0037M, 0.0037M and 0.0037M respectively) in 0.1 mm quartz cuvette. 10 accumulation scans.

Comparison of the ECD spectra of (X,S_S)-**3a** (left panel) and (Y,S_S)-**3a** (right panel) with the corresponding calculated spectra for (S_C,S_S) and (R_C,S_S), respectively is shown in Fig. SI-12.

ECD spectra calculation was carried out at TDDFT/CAM-B3LYP/TZVP/PCM(CH_3CN) level on optimized conformer geometries at B3LYP/TZVP/PCM(CH_3CN) level employed over the MM found structures as previously explained. The calculations for both diastereoisomers fit very well the experimental data, allowing us to predict the correct AC of the -C*H(CF_3)-NH- stereogenic carbon and, most important, consistently with the AC assigned by VCD analysis. In particular, the positive band at 290 nm of (X,S_S)-**3a** is predicted in sign by the ECD spectrum calculated for (S_C,S_S), while the corresponding negative band of (Y,S_S)-**3a** is in agreement with the calculated spectrum of (R_C,S_S). On the other hand it is also worth noting that 220 nm negative band allied to sulfoxide n→π* transition and the partial positive CE at ca. 185 nm preserve their sign in both calculated spectra, as expected. In conclusion, ECD analysis unambiguously confirms the AC assignment of the stereogenic carbon deduced by VCD investigation, that is to say: $X = S$ and $Y = R$.

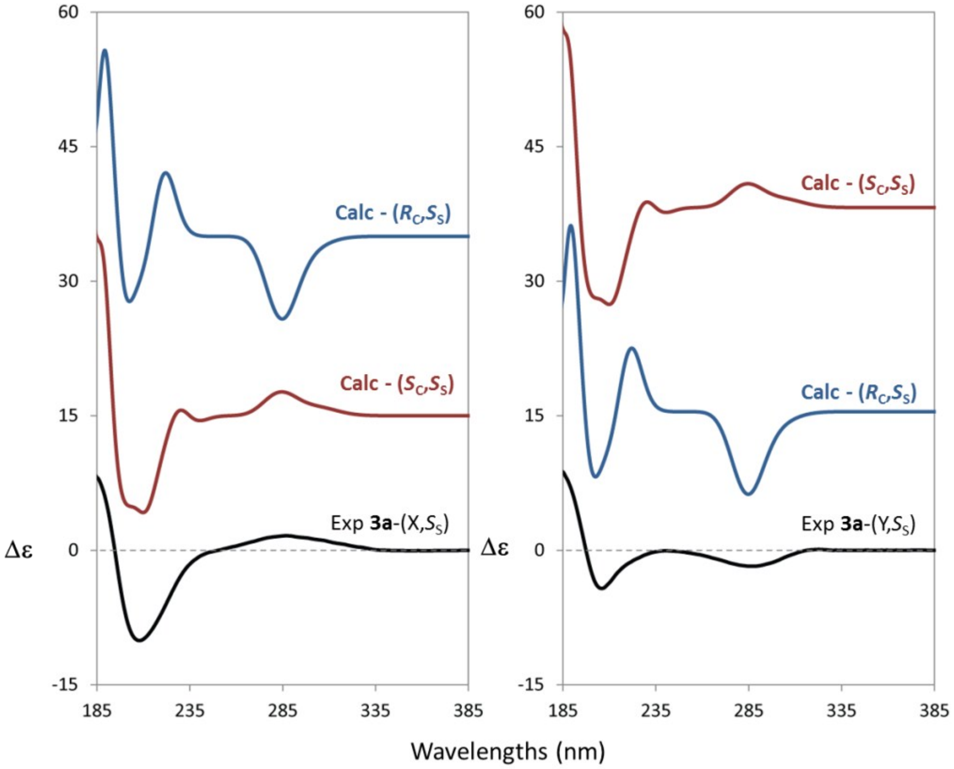

Figure SI-12. Experimental ECD of (X,S_S)-**3a** (left panel) and (Y,S_S)-**3a** (right panel), reported as semi-difference, compared with both calculated (S_C,S_S) and (R_C,S_S) diastereomers (as Boltzmann weighed average) at CAM-B3LYP/TZVP/PCM (CH_3CN) level, 50 first excited states and 0.2 eV wide Gaussian bands.

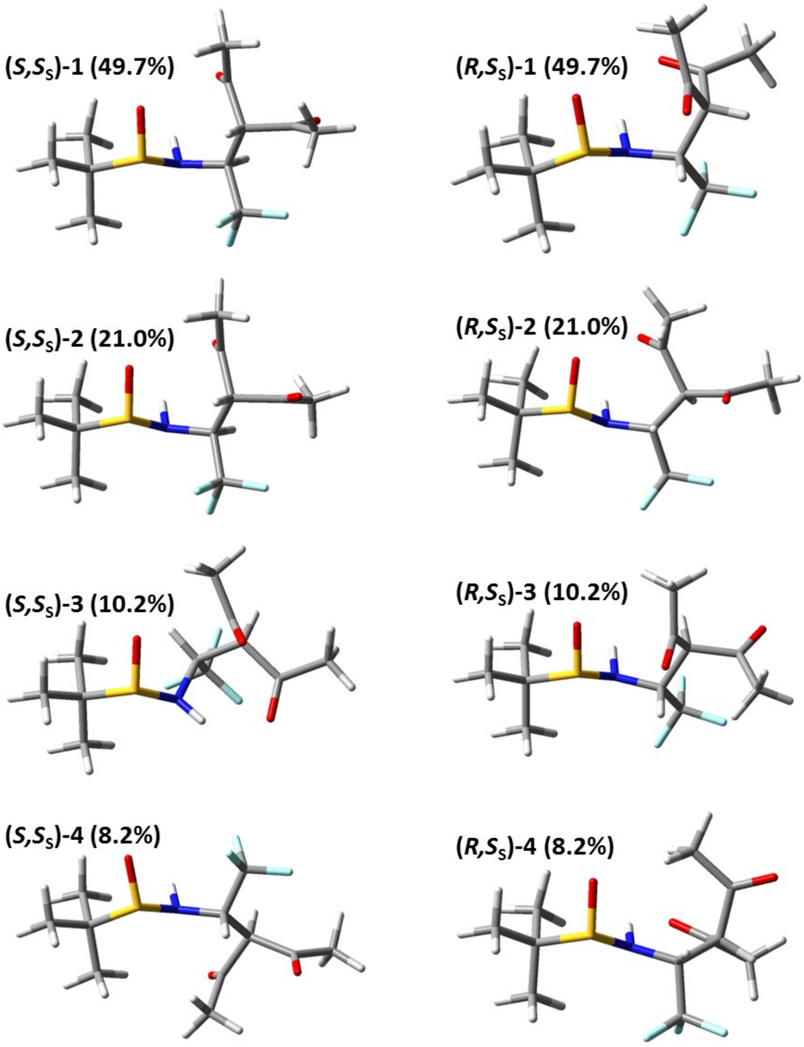

Figure SI-13. Calculated first four conformers of (S_C,S_S)-**3a** (left) and (R_C,S_S)-**3a** (right) diastereomers at the M062X/TZVP/PCM (CH_3CN) level. Relative populations in brackets.

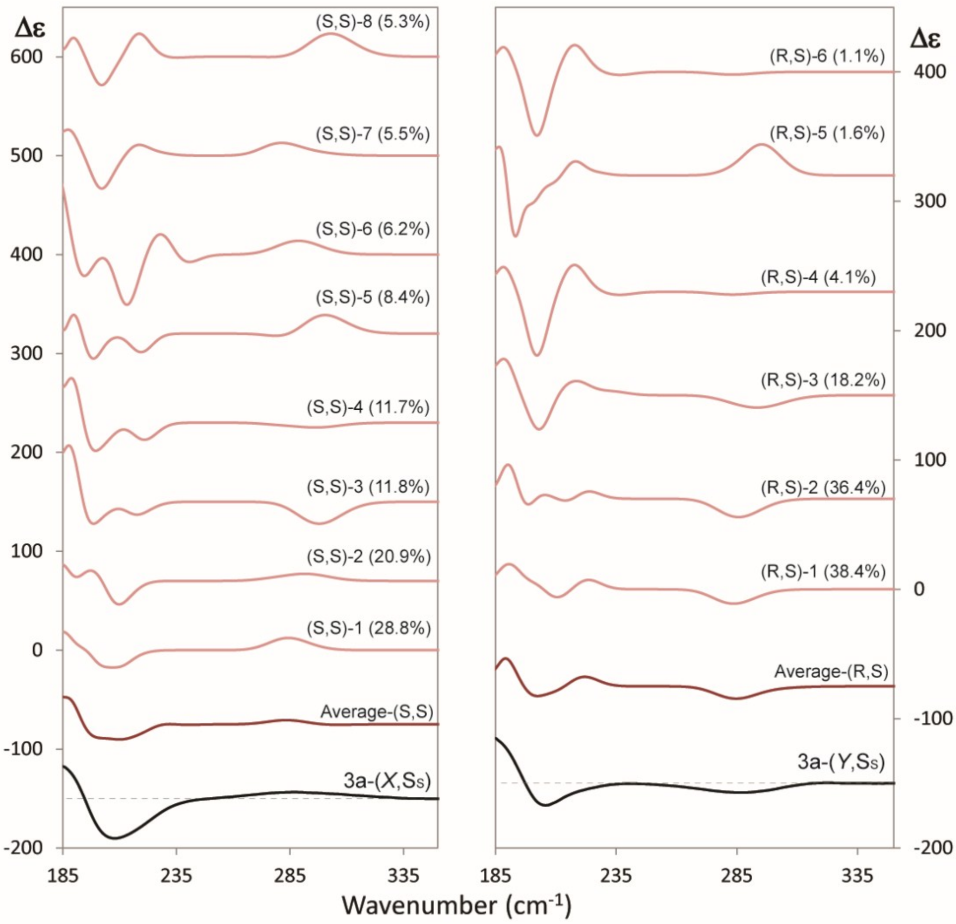

Figure SI-14. Calculated ECD spectra of first eight conformers (98.6% of overall population) of (S_C,S_S)-**3a** (left) and of first six conformers of (R_C,S_S)-**3a** (99.8% of overall population), compared with experimental and Boltzmann's averaged calculated spectra. Relative population percentages are reported in brackets. Calculations were performed at DFT/CAM-B3LYP/TZVP/PCM (CH_3CN). 50 first excited states and 0.2 eV wide Gaussian bands.

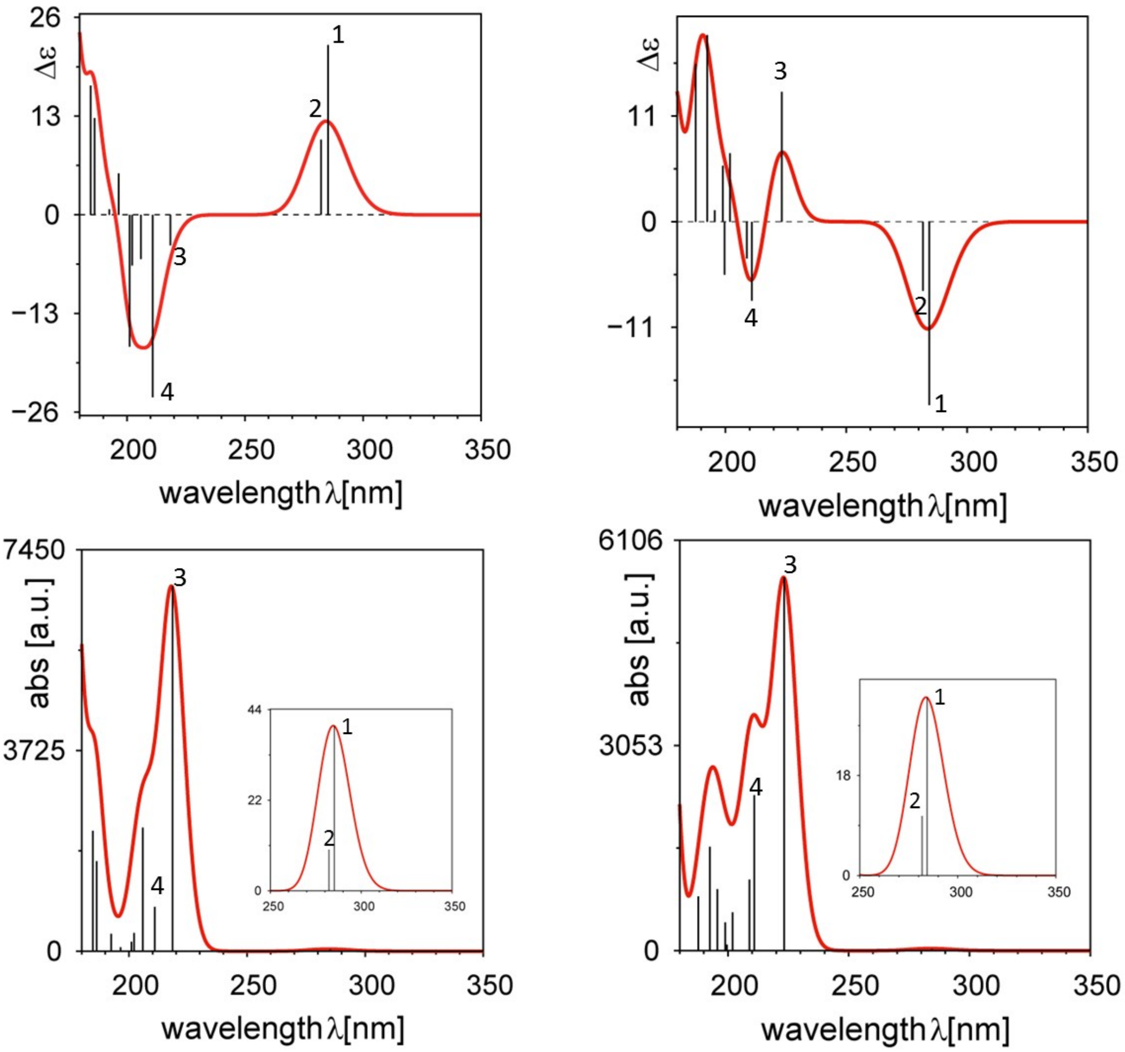

Figure SI-15. Calculated ECD and UV spectra for the first most populated conformers of (S_C,S_S)-**3a** (left) and of (R_C,S_S)-**3a** (right). Stick spectra superimposed for the analysis carried out in Figure SI-16. Calculations were performed at DFT/CAM-B3LYP/TZVP/PCM (CH_3CN). 50 first excited states and 0.2 eV wide Gaussian bands.

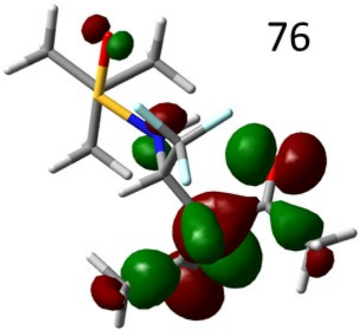

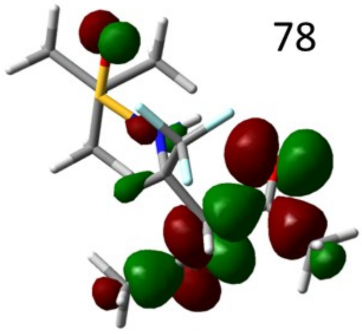

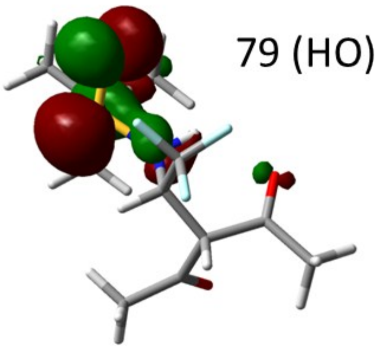

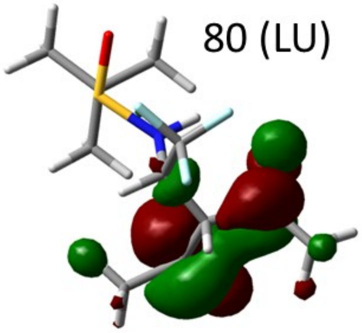

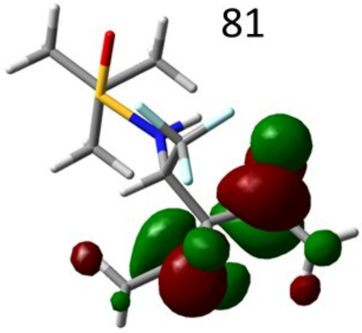

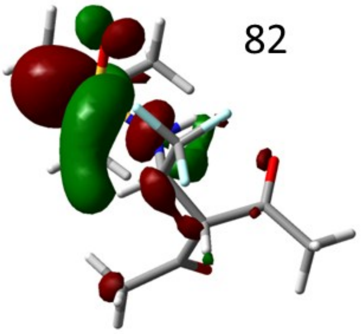

Transition SS-1	wavelength (nm)	osc. Strength	rot. Strength	Description
1	275.16	0.0003	15.56	78→80; 76→81; 78→81
2	272.19	0.0001	6.87	76→81; 78→81
3	208.37	0.0739	-2.64	79→82
4	200.91	0.0088	-16.75	79→80
Transition RS-1				
1	274.39	0.0003	-14.69	78→80; 76→81; 78→81
2	271.8	0.0001	-5.53	76→81; 78→81
3	213.26	0.0618	10.39	79→82
4	200.94	0.027	-6.32	79→80

Table SI-5. Molecular orbital analysis of the first four transitions of (S_C,S_S)-**3a** and of (R_C,S_S)-**3a** (wavelengths, oscillator strengths, rotatory strengths added). For definition of orbitals see figures above the table for the (S_C,S_S)-**3a** case (involved orbitals for (R_C,S_S)-**3a** are the same, *mutatis mutandis*). Calculations were performed at DFT/CAM-B3LYP/TZVP/PCM (CH_3CN).

References

1. M. J. Frisch, G. W. Trucks, H. B. Schlegel, G. E. Scuseria, M. A. Robb, J. R. Cheeseman, G. Scalmani, V. Barone, B. Mennucci, G. A. Petersson et al., Gaussian. Gaussian 09, Revision A.02; Gaussian, Inc.: Wallingford, CT, USA, 2009.
2. J. Tomasi, B. Mennucci and R. Cammi, *Chem. Rev.* 2005, **105**, 2999–3094.

3. L. A. Nafie, “Vibrational Optical Activity-Principles and Application”, Wiley: New York, NY, USA, 2011.

4. P.L. Polavarapu, “Chiroptical Spectroscopy Fundamentals and Applications”, CRC Publisher: Boca Raton, FL, USA, 2017.

5. P. J. Stephens, *J. Phys. Chem.* 1985, **89**, 748–750.

6. N. M. Kreienborg and C. Merten, *Phys. Chem. Chem. Phys.* 2018, DOI: 10.1039/C8CP02395F

7. G. Mazzeo, G. Longhi, S. Abbate, M. Palomba, L. Bagnoli, F. Marini, C. Santi, J. L. Han, V. A. Soloshonok, E. Di Crescenzo and R. Ruzziconi, *Org. Biomol. Chem.* 2017, **15**, 3930–3937.

8. G. Mazzeo, G. Longhi, S. Abbate, F. Buonerba and R. Ruzziconi, *Eur. J. Org. Chem*. 2014, 7353–7363.

9. T. Kuppens, W. Langenaeker, J. P. Tollenaere and P. Bultinck, *J. Phys. Chem. A* 2003, **107**, 542–553

10. J. Shen, C. Zhu, S. Reiling and R. Vaz, *Spectrochim. Acta*, *Part A* 2010, **A76**, 418–422.

11. G. Mazzeo, A. Cimmino, M. Masi, G. Longhi, L. Maddau, M. Memo, A. Evidente and S. Abbate, *J. Nat. Prod.* 2017, **80**, 2406–2415.

12. M. Miceli, A. Mazziotta, C. Palumbo, E. Roma, E. Tosi, G. Longhi, S. Abbate, P. Lupattelli, G. Mazzeo and T. Gasperi, *Molecules* 2018, **23**, doi.org/10.3390/molecules23020438.

13. S. Vergura, E. Santoro, M. Masi, A. Evidente, P. Scafato, S. Superchi, G. Mazzeo, G. Longhi and S. Abbate, *Fitoterapia* 2018, **129**, 78–84.

14. Y. L. Frolov, L. M. Sinegovskaya, N. K. Gusarova, G. G. Efremova and B. A. Trofimov, *Russ. Chem. Bull.* 1978, **27**, 901–904.

15. C. Rosini, M. Donnoli and S. Superchi, *Chem. Eur. J.* 2001, **7**, 72–79.

16. R. Berardozzi, C. A. Guido, M. A. Capozzi, C. Cardellicchio, L. Di Bari and G. Pescitelli, *Eur. J. Org. Chem.* **2015**, 5554–5562.

17. E. Giorgio, R. G. Viglione, R. Zanasi and C. Rosini, *J. Am. Chem. Soc.* 2004, **126**, 12968–12976.